A novel computational pipeline for *var* gene expression augments the discovery of changes in the *Plasmodium falciparum* transcriptome during transition from *in vivo* to short-term *in vitro* culture

Clare Andradi-Brown[1,2,3], Jan Stephan Wichers-Misterek[4-6], Heidrun von Thien[4-6], Yannick D. Höppner[4-6], Judith A. M. Scholz[4], Helle Hansson[7,8], Emma Filtenborg Hocke[7,8], Tim-Wolf Gilberger[4-6], Michael F. Duffy[9], Thomas Lavstsen[7,8], Jake Baum[2,10], Thomas D. Otto[11*], Aubrey J. Cunnington[1,3*¥], Anna Bachmann[4-6,12*¥]

[1] Section of Paediatric Infectious Disease, Department of Infectious Disease, Imperial College London, UK
[2]Department of Life Sciences, Imperial College London, South Kensington, London, SW7 2AZ, UK
[3]Centre for Paediatrics and Child Health, Imperial College London, UK
[4]Bernhard Nocht Institute for Tropical Medicine, Bernhard-Nocht-Strasse 74, 20359 Hamburg, Germany
[5]Centre for Structural Systems Biology, Hamburg, Germany, Notkestraße 85, 22607 Hamburg, Germany
[6]Biology Department, University of Hamburg, Hamburg, Germany
[7]Center for Medical Parasitology, Department of Immunology and Microbiology, University of Copenhagen, 2200 Copenhagen, Denmark
[8]Department of Infectious Diseases, Copenhagen University Hospital, 2200 Copenhagen, Denmark
[9]Department of Microbiology and Immunology, University of Melbourne, Melbourne/Parkville VIC 3052, Australia
[10]School of Biomedical Sciences, Faculty of Medicine & Health, UNSW, Kensington, Sydney, 2052, Australia
[11]School of Infection & Immunity, MVLS, University of Glasgow, UK
[12]German Center for Infection Research (DZIF), partner site Hamburg-Borstel-Lübeck-Riems, Germany
*Equal contribution
¥To whom correspondence should be addressed

Corresponding authors:
Aubrey Cunnington, Section of Paediatric Infectious Disease, Department of Infectious Disease, Imperial College London, Norfolk Place, W2 1PG, London, UK. a.cunnington@imperial.ac.uk
Anna Bachmann, Bernhard Nocht Institute for Tropical Medicine, Bernhard-Nocht-Strasse 74, 20359 Hamburg, Germany. bachmann@bni-hamburg.de

Abstract

The pathogenesis of severe *Plasmodium falciparum* malaria involves cytoadhesive microvascular sequestration of infected erythrocytes, mediated by *P. falciparum* erythrocyte membrane protein 1 (PfEMP1). PfEMP1 variants are encoded by the highly polymorphic family of *var* genes, the sequences of which are largely unknown in clinical samples. Previously, we published new approaches for *var* gene profiling and classification of predicted binding phenotypes in clinical *P. falciparum* isolates (Wichers *et al.*, 2021), which represented a major technical advance. Building on this, we report here a novel method for *var* gene assembly and multidimensional quantification from RNA-sequencing that outperforms the earlier approach of Wichers *et al*., 2021 on both laboratory and clinical isolates across a combination of metrics. Importantly, the tool can interrogate the *var* transcriptome in context with the rest of the transcriptome and can be applied to enhance our understanding of the role of *var* genes in malaria pathogenesis. We applied this new method to investigate changes in *var* gene expression through early transition of parasite isolates to *in vitro* culture, using paired sets of *ex vivo* samples from our previous study, cultured for up to three generations. In parallel, changes in non-polymorphic core gene expression were investigated. Modest but unpredictable *var* gene switching and convergence towards *var2csa* were observed in culture, along with differential expression of 19% of the core transcriptome between paired *ex vivo* and generation 1 samples. Our results cast doubt on the validity of the common practice of using short-term cultured parasites to make inferences about *in vivo* phenotype and behaviour.

Introduction

Malaria is a parasitic life-threatening disease caused by species of the *Plasmodium* genus. In 2021, there were an estimated 619,000 deaths due to malaria, with children under 5 accounting for 77% of these (WHO, 2022). *Plasmodium falciparum* causes the greatest disease burden and most severe outcomes, but our efforts to combat the disease are challenged by its complex life cycle and its sophisticated immune evasion strategies. *P. falciparum* has several highly polymorphic variant surface antigens (VSA) encoded by multi-gene families, with the best studied high molecular weight *Plasmodium falciparum* erythrocyte membrane protein 1 (PfEMP1) family of proteins known to play a major role in the pathogenesis of malaria (Leech *et al.*, 1984, Wahlgren *et al.*, 2017). About 60 polymorphic *var* genes per parasite genome encode different PfEMP1 variants, which are exported to the surface of parasite-infected erythrocytes, where they mediate cytoadherence to host endothelial cells (Leech *et al.*, 1984, Su *et al.*, 1995, Smith *et al.*, 1995, Baruch *et al.*, 1995, Rask *et al.*, 2010). *Var* genes are expressed in a mutually exclusive pattern, resulting in each parasite expressing only one *var* gene, and therefore one PfEMP1 protein, at a time (Scherf *et al.*, 1998). Due to the exposure of PfEMP1 proteins to the host immune system, switching expression between the approximately 60 *var* genes in the genome is an effective immune evasion strategy, which can result in selection and dominance of parasites expressing particular *var* genes within each host (Smith *et al.*, 1995).

Despite their sequence polymorphism, *var* genes could be classified into four categories (A, B, C, and E) according to their chromosomal location, transcriptional direction, type of 5'-upstream sequence (UPSA–E), and encoded protein domains with associated binding phenotype (Figure 1) (Lavstsen *et al.*, 2003, Kraemer & Smith, 2003, Kyes *et al.*, 2007, Rask *et al.*, 2010). PfEMP1 proteins have up to 10 extracellular domains, with the N-terminal domains forming a semi-conserved head structure complex typically containing the N-terminal segment (NTS), a Duffy binding-like domain of class α (DBLα) coupled to a cysteine-rich interdomain region (CIDR). C-terminally to this head structure, PfEMP1 proteins exhibit a varying but semi-ordered composition of additional DBL and CIDR domains of different subtypes (Figure 1c). The PfEMP1 family divides into three main groups based on the receptor specificity of the N-terminal CIDR domain: (i) PfEMP1 proteins with CIDRα1 domains bind endothelial protein C receptor (EPCR), while (ii) PfEMP1 proteins with CIDRα2–6 domains bind CD36 and (iii) the atypical VAR2CSA PfEMP1 proteins bind placental chondroitin sulphate A (CSA) (Salanti *et al.*, 2004). In addition to these, a subset of PfEMP1 proteins have N-terminal CIDRβ/γ/δ domains of unknown function. This functional diversification correlates with the genetic organization of the *var* genes. Thus, UPSA *var* genes encode PfEMP1 proteins with domain sub-variants NTSA-DBLα1-CIDRα1/β/γ/δ, whereas UPSB and UPSC *var* genes encode PfEMP1 proteins with NTSB-DBLα0-CIDRα2–6. One exception to this rule is the B/A chimeric *var* genes, which encode NTSB-DBLα2-CIDRα1 domains. The different receptor binding specificities are associated with different clinical outcomes of infection. Pregnancy-associated malaria is linked to parasites expressing VAR2CSA, whereas parasites expressing EPCR-binding PfEMP1 are linked to severe malaria and parasites expressing CD36-binding PfEMP1 are linked to uncomplicated malaria (Turner *et al.*, 2013, Lavstsen *et al.*, 2012, Avril *et al.*, 2012, Claessens *et al.*, 2012, Tonkin-Hill *et al.*, 2018, Wichers *et al.*, 2021). The clinical relevance of PfEMP1 proteins with unknown binding phenotypes of the N-terminal head structure and C-terminal PfEMP1 domains is largely unknown, albeit specific interactions with endothelial receptors and plasma proteins have been described (Tuikue Ndam *et al.*, 2017, Quintana *et al.*, 2019, Stevenson *et al.*, 2015). Each parasite genome carries a similar repertoire of *var* genes, which in addition to the described variants include a highly conserved *var1* variant of either type 3D7 or IT, which in most genomes occurs with a truncated or absent exon 2. Also, most genomes carry the unusually small and highly conserved *var3* genes, of unknown function (Figure 1c) (Otto *et al.*, 2019).

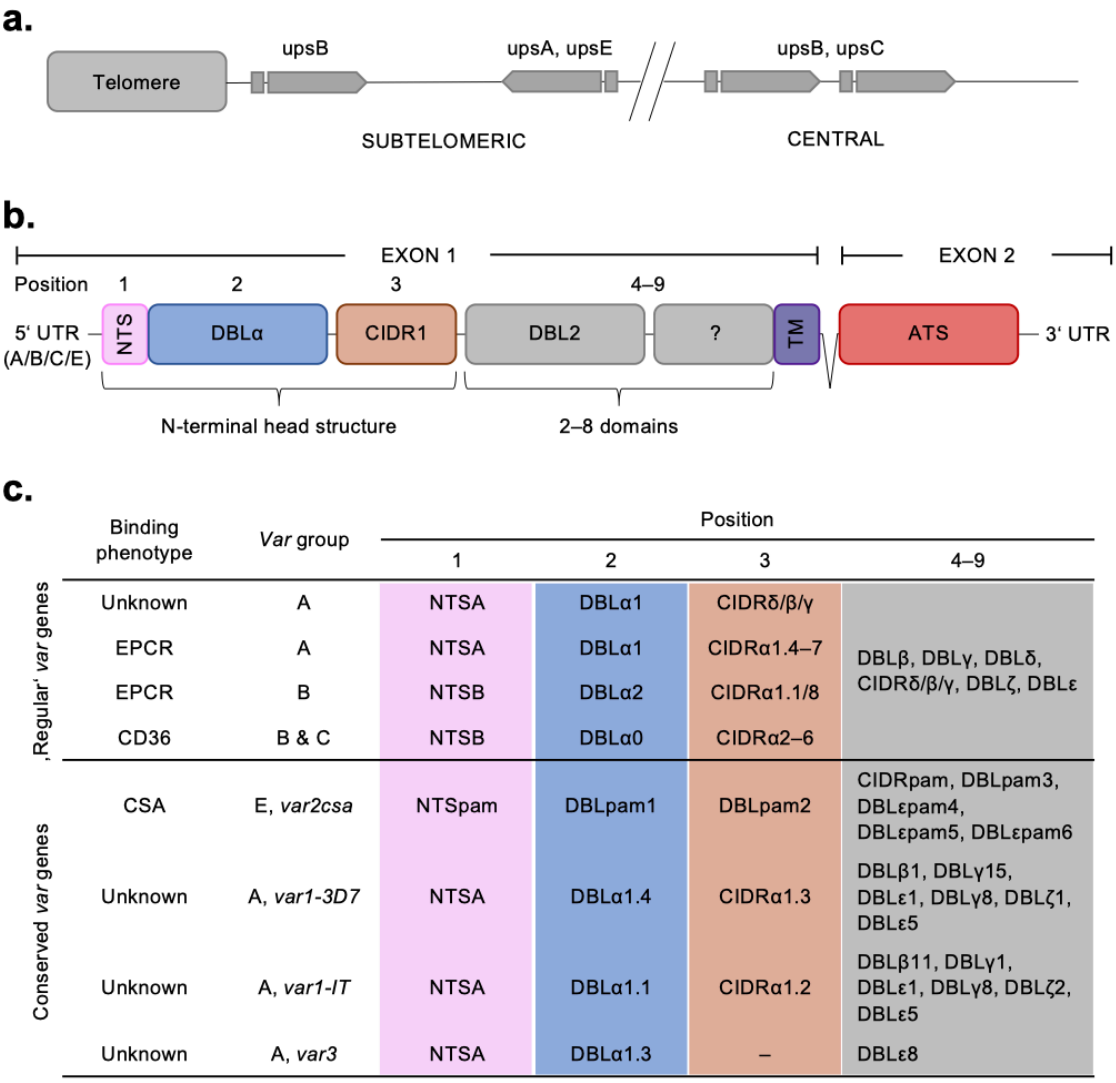

Figure 1: Summary of the *var* chromosomal location, *var* gene, PfEMP1 protein structure, and PfEMP1 binding phenotypes. a) Chromosomal position and transcriptional direction (indicated by arrows) of the different *var* gene groups, designated by the respective type of upstream sequence (Kraemer and Smith et al., 2003, Lavstsen et al., 2003). **b)** Structure of the *var* gene which encodes the PfEMP1 protein. The *var* gene is composed of two exons, the first, around 3–9.4 kb, encodes the highly variable extracellular region and the transmembrane region (TM) of PfEMP1. Exon 2 is shorter with about 1.2 kb and encodes a semi-conserved intracellular region (acidic terminal segment, ATS). The PfEMP1 protein is composed of an N-terminal segment (NTS), followed by a variable number of Duffy binding-like (DBL) domains and cysteine-rich interdomain regions (CIDR) (Rask et al., 2010). **c)** Summary of PfEMP1 proteins encoded in the parasite genome, their composition of domain subtypes and associated N-terminal binding phenotype. Group A and some B proteins have an EPCR-binding phenotype; the vast majority of group B and C PfEMP1 proteins bind to CD36. Group A proteins also include those that bind a yet unknown receptor, as well as VAR1 and VAR3 variants with unknown function and binding phenotype. VAR2CSA (group E) binds placental CSA.

91 Comprehensive characterisation and quantification of *var* gene expression in field samples have been
92 complicated by biological and technical challenges. The extreme polymorphism of *var* genes precludes a
93 reference *var* sequence.*Var* genes can be lowly expressed or not expressed at all, contain repetitive domains
94 and can have large duplications (Otto *et al.*, 2019). Consequently, most studies relating *var* gene expression
95 to severe malaria have relied on primers with restricted coverage of the *var* family, use of laboratory-adapted
96 parasite strains or have predicted the downstream sequence from DBLα domains (Sahu *et al.*, 2021, Storm *et*
97 *al.*, 2019, Shabani *et al.*, 2017, Mkumbaye *et al.*, 2017, Kessler *et al.*, 2017, Bernabeu *et al.*, 2016, Jespersen
98 *et al.*, 2016, Lavstsen *et al.*, 2012). This has resulted in incomplete *var* gene expression quantification and the
99 inability to elucidate specific or detect atypical *var* sequences. RNA-sequencing has the potential to overcome
100 these limitations and provide a better link between *var* expression and PfEMP1 phenotype in *in vitro* assays,
101 co-expression with other genes or gene families and epigenetics. While approaches for *var* assembly and
102 quantification based on RNA-sequencing have recently been proposed (Wichers *et al.*, 2021; Stucke et al.,

2021; Andrade et al., 2020; Tonkin-Hill *et al.*, 2018, Duffy et al., 2016), these still produce inadequate assembly of the biologically important N-terminal domain region, have a relatively high number of misassemblies and do not provide an adequate solution for handling the conserved *var* variants (Table S1).

Plasmodium parasites from human blood samples are often adapted to or expanded through *in vitro* culture to provide sufficient parasites for subsequent investigation of parasite biology and phenotype (Brown & Guler, 2020). This is also the case for several studies assessing the PfEMP1 phenotype of parasites isolated from malaria-infected donors (Pickford *et al.*, 2021, Joste *et al.*, 2020, Storm *et al.*, 2019, Tuikue Ndam *et al.*, 2017, Bruske *et al.*, 2016, Claessens *et al.*, 2012, Lavstsen *et al.*, 2005, Jensen *et al.*, 2004, Kirchgatter & Portillo Hdel, 2002, Dimonte *et al.*, 2016, Hoo *et al.*, 2019). However, *in vitro* conditions are considerably different to those found *in vivo,* for example in terms of different nutrient availability and lack of a host immune response (Brown & Guler, 2020). Previous studies found inconsistent results in terms of whether *var* gene expression is impacted by culture and, if so, which *var* groups were the most affected (Zhang *et al.*, 2011, Peters *et al.*, 2007). Similar challenges apply to the understanding of changes in *P. falciparum* non-polymorphic core genes in culture, with the focus previously being on long-term laboratory adapted parasites (Claessens *et al.*, 2017, Mackinnon *et al.*, 2009). Consequently, direct interpretation of a short-term cultured parasite's transcriptome remains a challenge. It is fundamental to understand *var* genes in context with the parasite's core transcriptome. This could provide insights into *var* gene regulation and phenomena such as the proposed lower level of *var* gene expression in asymptomatic individuals (Almelli *et al.*, 2014, Andrade *et al.*, 2020).

Here we present an improved method for assembly, characterization, and quantification of *var* gene expression from RNA-sequencing data. This new approach overcomes previous limitations and outperforms current methods, enabling a much greater understanding of the *var* transcriptome. We demonstrate the power of this new approach by evaluating changes in *var* gene expression of paired samples from clinical isolates *of P. falciparum* during their early transition to *in vitro* culture*,* across several generations. The use of paired samples, which are genetically identical and hence have the same *var* gene repertoire, allows validation of assembled transcripts and direct comparisons of expression. We complement this with a comparison of changes which occur in the non-polymorphic core transcriptome over the same transition into culture. We find a background of modest changes in *var* gene expression with unpredictable patterns of *var* gene switching, favouring an apparent convergence towards *var2csa* expression. More extensive changes were observed in the core transcriptome during the first cycle of culture, suggestive of a parasite stress response.

Results

To extend our ability to characterise *var* gene expression profiles and changes over time in clinical *P. falciparum* isolates, we set out to improve current assembly methods. Previous methods for assembling *var* transcripts have focussed on assembling whole transcripts (Tonkin-Hill *et al.*, 2018, Wichers *et al.*, 2021, Guillochon *et al.*, 2022, Andrade *et al.*, 2020). However, due to the diversity within PfEMP1 domains, their associations with disease severity and the fact different domain types are not inherited together, a method focussing on domain assembly first was developed. In addition, a novel whole transcript approach, using a different *de novo* assembler, was developed and their performance compared to the method of Wichers *et al.* (hereafter termed "original approach", Figure 2) (Wichers *et al.*, 2021). The new approaches made use of the MalariaGEN *P. falciparum* dataset, which led to the identification of additional multi-mapping non-core reads (a median of 3,955 reads per sample) prior to *var* transcript assembly (MalariaGen *et al.*, 2021). We incorporated read error correction and improved large scaffold construction with fewer misassemblies (see Methods). We then applied this pipeline to paired *ex vivo* and short-term *in vitro* cultured parasites to enhance our understanding of the impact of short-term culturing on the *var* transcriptome (Figure 3). The *var* transcriptome was assessed at several complementary levels: first, changes in the dominantly expressed *var* gene and the homogeneity of the *var* expression profile in paired samples were investigated; second, changes in *var* domain expression through culture were assessed; and third, *var* group and global *var* gene expression changes were evaluated. All these analyses on *var* expression were accompanied by analysis of the core transcriptome at the transition to short-term culture.

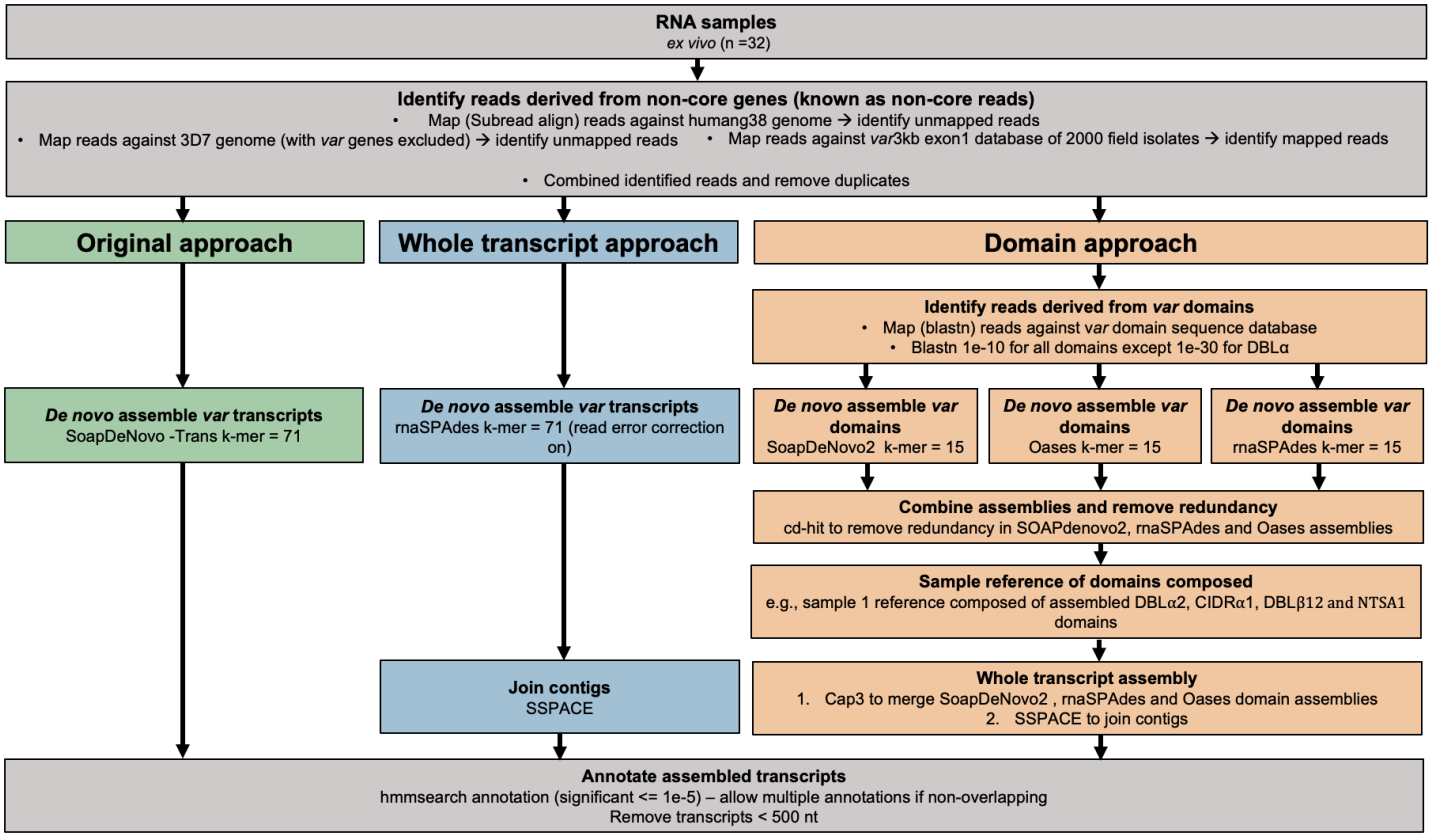

Figure 2: Overview of novel computational pipelines for assembling *var* transcripts. The original approach (green) used SoapDeNovo-Trans (k=71) to perform whole *var* transcript assembly. The whole transcript approach (blue) focused on assembling whole *var* transcripts from the non-core reads using rnaSPAdes (k = 71). Contigs were then joined into longer transcripts using SSPACE. The domain approach (orange) assembled *var* domains first and then joined the domains into whole transcripts. Domains were assembled separately using three different *de novo* assemblers (SoapDeNovo2, Oases and rnaSPAdes). Next, a reference of assembled domains was composed and cd-hit (at sequence identity = 99%) was used to remove redundant sequences. Cap3 was used to merge and extend domain assemblies. Finally, SSPACE was used to join domains together. HMM models built on the Rask *et al.*, 2010 dataset were used to annotate the assembled transcripts (Rask *et al.*, 2010). The most significant alignment was taken as the best annotation for each region of the assembled transcript (significance <= 1e-5) identified using cath-resolve-hits0. Transcripts < 500nt were removed. A *var* transcript was selected if it contained at least one significantly annotated domain (in exon 1). *Var* transcripts that encoded only the more conserved exon 2 (ATS domain) were discarded. The three pipelines were run on the 32 malaria patient *ex vivo* samples from Wichers *et al.*, 2021 (Wichers *et al.*, 2021).

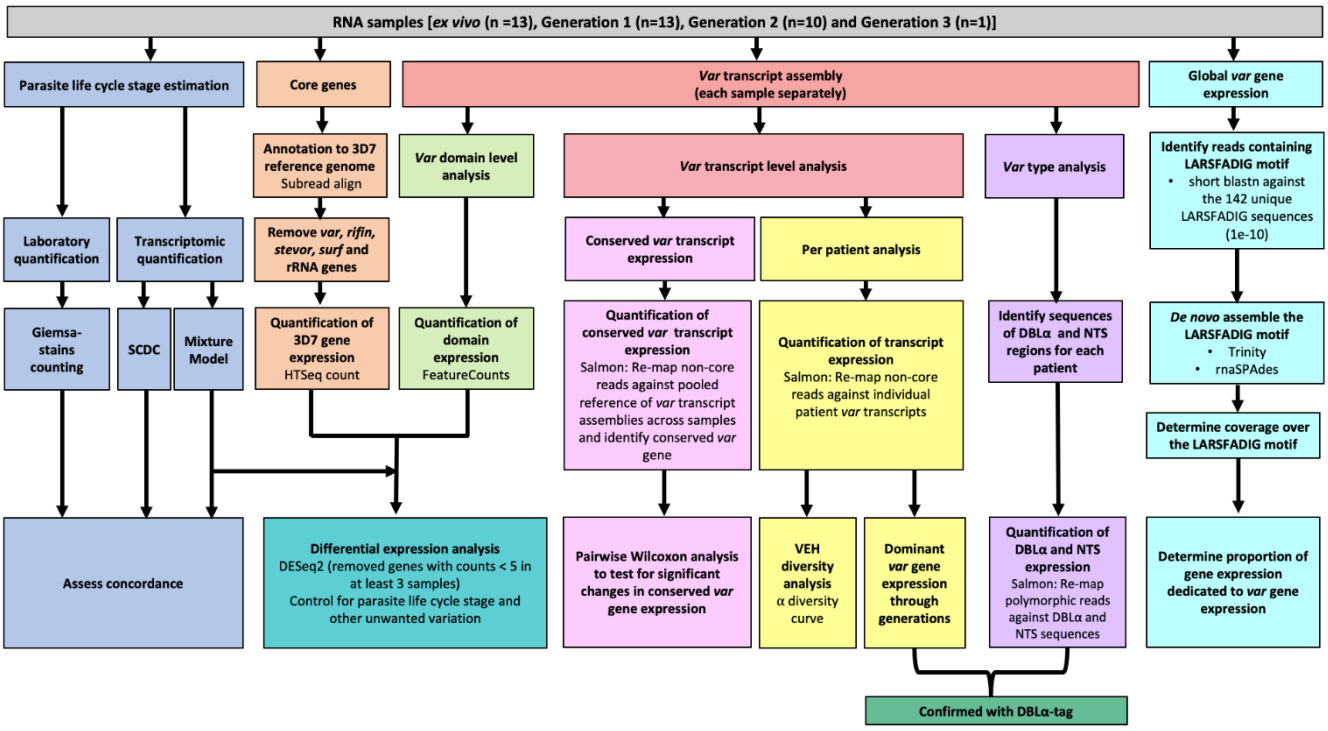

Figure 3: Summary of analyses of *var* and core gene transcriptome changes in paired *ex vivo* and short-term *in vitro* cultured parasites. From a total of 13 parasite isolates, the *ex vivo* samples (Wichers *et al.*, 2021) and the corresponding *in vitro*-cultured parasites of the first (n=13), second (n=10) and third (n=1) replication cycle were analysed by RNA sequencing. The expression of non-polymorphic core genes and polymorphic *var* genes was determined in different analysis streams: (1) Non-polymorphic core gene reads were mapped to the 3D7 reference genome, expression was quantified using HTSeq and differential expression analysis performed (orange); (2) Non-core reads were identified, whole transcripts were assembled with rnaSPAdes, expression of both *var* transcripts (red) and domains (light green) was quantified, and *var* domain differential expression analysis was performed. "Per patient analysis" (yellow) represents combining all assembled *var* transcripts for samples originating from the same *ex vivo* sample only. For each conserved *var* gene (*var1-3D7*, *var1-IT*, *var2csa* and *var3*) all significantly assembled conserved *var* transcripts were identified and put into a combined reference (pink). The normalised counts for each conserved gene were summed. Non-core reads were mapped to this and DESeq2 normalisation performed. *Var* type (group A vs group B and C) expression (purple) was quantified using the DBLα and NTS assembled sequences and differences across generations were assessed. Total *var* gene expression (turquoise) was quantified by assembling and quantifying the coverage over the highly conserved LARSFADIG motif, with the performance of assembly using Trinity and rnaSPAdes assessed. DBLα-tag data was used to confirm the results of the dominant *var* gene expression analysis and the *var* type analysis (dark green). *Var* expression homogeneity (VEH) was analysed at the patient level (α diversity curves). All differential expression analyses were performed using DESeq2.To ensure a fair comparison of samples, which may contain different proportions of life cycle stages, the performance of two different *in silico* approaches was evaluated by counting Giemsa-stained thin blood smears (blue).

Improving *var* transcript assembly, annotation and quantification

A laboratory and a clinical dataset were used to assess the performance of the different *var* assembly pipelines (Figure 2). The laboratory dataset was a *P. falciparum* 3D7 time course RNA-sequencing dataset (European nucleotide archive (ENA): PRJEB31535) (Wichers *et al.*, 2019). The clinical dataset contained samples from 32 adult malaria patients, hospitalised in Hamburg, Germany (National Center for Biotechnology Information (NCBI) BioProject ID: PRJNA679547). Fifteen were malaria naïve and 17 were previously exposed to malaria. Eight of the malaria naïve patients went on to develop severe malaria and 24 had non-severe malaria (Wichers *et al.*, 2021).

Our i) new whole transcript approach, ii) domain assembly approach, and iii) modified version of the original approach (see material and methods) were first applied to a *P. falciparum* 3D7 time course RNA-sequencing dataset to benchmark their performance (Wichers *et al.*, 2019) (Figure 2 – Figure supplement 1). The whole transcript approach performed best, achieving near perfect alignment scores for the dominantly expressed *var* gene (Figure 2 – Figure supplement 1a). The domain and the original approach produced shorter contigs and required more contigs to assemble the *var* transcripts at the 8 and 16 hour post-invasion time points, when *var* gene expression is maximal (Figure 2 – Figure supplement 1c, f, g and h). However, we found high accuracies (> 0.95) across all approaches, meaning the sequences we assembled were correct (Figure 2 – Figure supplement 1b). The whole transcript approach also performed the best when assembling the lower expressed *var* genes (Figure 2 – Figure supplement 1e) and produced the fewest *var* chimeras compared to

172 the original approach on *P. falciparum* 3D7. Fourteen misassemblies were observed with the whole transcript
173 approach compared to 19 with the original approach (Table S2). This reduction in misassemblies was
174 particularly apparent in the ring-stage samples.
175
176 Next, the assembled transcripts produced from the original approach of Wichers *et al.*, 2021 were compared
177 to those produced from our new whole transcript and domain assembly approaches for *ex vivo* samples from
178 German travellers. Summary statistics are shown in Table 1. The whole transcript approach produced the
179 fewest transcripts, but of greater length than the domain approach and the original approach (Figure 2 –
180 Figure supplement 2). The whole transcript approach also returned the largest N50 score (more than doubling
181 the N50 of the original approach), which means that it was the most contiguous assembly produced.
182 Remarkably, with the new whole transcript method, we observed a significant decrease (2 vs 336) in clearly
183 misassembled transcripts with, for example, an N-terminal domain at an internal position.
184
185 When genome sequencing is not available, concordance of different *var* profiling approaches can support the
186 validation of an approach. Here, the same methods used in the original analysis were applied for quantifying
187 the expression of the assembled *var* transcripts and domains. This suggests any concordance in expression
188 estimates likely reflects concordance at the domain annotation level. The original approach and the new
189 whole transcript approach gave similar results for domain expression in each sample with greater correlation
190 in results observed between the highly expressed domains (Figure 2 – Figure supplement 3). As expected,
191 comparable results were also seen for the differentially expressed transcripts identified in the original analysis
192 between the naïve vs pre-exposed and severe vs non-severe comparisons, respectively (Figure 2 – Figure
193 supplement 4).

Table 1: Statistics for the different approaches used to assemble the *var* transcripts. *Var* assembly approaches were applied to malaria patient *ex vivo* samples (n=32) from (Wichers *et al.*, 2021) and statistics determined. Given are the total number of assembled *var* transcripts longer than 500 nt containing at least one significantly annotated *var* domain, the maximum length of the longest assembled *var* transcript in nucleotides and the N50 value, respectively. The N50 is defined as the sequence length of the shortest *var* contig, with all *var* contigs greater than or equal to this length together accounting for 50% of the total length of concatenated *var* transcript assemblies. Misassemblies represents the number of misassemblies for each approach. **Number of misassemblies were not determined for the domain approach due to its poor performance in other metrics.

	Number of contigs ≥500nts	Maximum length (nt)	Average contig length (nt)	N50	Number of misassemblies
Original approach	6,441	10,412	1,621	2,302	336
Domain approach	4,691	5,003	954	1,088	NA**
Whole transcript approach	3,011	12,586	2,771	5,381	2

194
195 Overall, the new whole transcript approach performed the best on the laboratory 3D7 dataset (ENA:
196 PRJEB31535) (Wichers *et al.*, 2019), had the greatest N50, the longest *var* transcripts and produced
197 concordant results with the original analysis on the clinical *ex vivo* samples (NCBI: PRJNA679547) (Wichers *et*
198 *al.*, 2021). Therefore, it was selected for all subsequent analyses unless specified otherwise.
199
200 Establishing characterisation of *var* transcripts from *ex vivo* and *in vitro* samples
201 Of the 32 clinical isolates of *P. falciparum* from the German traveller dataset, 13 underwent one replication
202 cycle of *in vitro* culture, 10 of these underwent a second generation and one underwent a third generation
203 (Table 2). Most (9/13, 69%) isolates entering culture had a single MSP1 genotype, indicative of monoclonal
204 infections. All samples were sequenced with a high read depth, although the *ex vivo* samples had a greater
205 read depth than the *in vitro* samples (Table 2). Figure 3 shows a summary of the analysis performed.

Table 2: Summary of the clinical dataset used to analyze the impact of parasite culturing on gene expression. RNA-sequencing was performed on 32 malaria infected German traveler samples (Wichers *et al.*, 2021). The 32 *ex vivo* samples were used to compare the performance of the *var* assembly approaches. Parasites from 13 of these *ex vivo* samples underwent one cycle of *in vitro* replication, 10 parasite samples were also subjected to a second cycle of replication *in vitro*, and a single parasite isolate was also analyzed after a third cycle of replication. For the *ex vivo* vs short-term *in vitro* cultivation analysis only paired samples were used. The number of assembled *var* contigs represents results per sample using the whole transcript approach, and shows either the number of assembled *var* contigs significantly annotated as *var* gene and > =500nt in length, or the number of assembled *var* transcripts identified with a length >= 1500nt and containing at least 3 significantly annotated *var* domains. *PE; paired-end reads.

			Generation		
		***Ex vivo* (n=32)**	**1 (n=13)**	**2 (n=10)**	**3 (n=1)**
Malaria exposure (n)	**Naïve**	15	6	4	1
	Previously exposed	17	7	6	0
Malaria severity (n)	**Severe**	8	3	1	0
	Non-severe	24	10	9	1
Number of MSP1 genotypes (number of samples)	**1**	22	9	7	1
	2	4	0	0	0
	3	5	3	0	0
	4	1	1	0	0
Number of *P. falciparum* PE* reads (non-*var*) (median, IQR) (million of reads)		34.6 (27.0–36.5)	17.1 (12.9–18.0)	17.2 (12.9–19.1)	15.1
Number of non-core *P. falciparum* PE* reads (median, IQR) (million of reads)		5.05 (3.62–6.60)	1.16 (1.07–1.40)	1.29 (1.04–1.58)	0.91
Number of assembled *var* contigs in a sample (≥500nts) (whole transcript approach) (median, IQR)		53 (44–84)	61 (38–76)	71.5 (48.25–79.5)	75
Number of assembled *var* contigs in a sample (≥1,500nts and 3 sig. domain annotations) (whole transcript approach) (median, IQR)		20 (7–31)	15.5 (10–26)	15 (10.25–23.75)	18

To account for differences in parasite developmental stage within each sample, which are known to impact gene expression levels (Bozdech *et al.*, 2003), the proportions of life cycle stages were estimated using the mixture model approach of the original analysis (Tonkin-Hill *et al.*, 2018, Wichers *et al.*, 2021). As a complementary approach, single cell differential composition analysis (SCDC) with the Malaria Cell Atlas as a reference was also used to determine parasite age (Dong *et al.*, 2021, Howick *et al.*, 2019). SCDC and the mixture model approaches produced concordant estimates that most parasites were at ring stage in all *ex vivo* and *in vitro* samples (Figure 3 – Figure supplement 1a,b). Whilst there was no significant difference in ring stage proportions across the generations, we observed a slight increase in parasite age in the cultured samples. Overall, there were more rings and early trophozoites in the *ex vivo* samples compared to the cultured parasite samples and an increase of late trophozoite, schizont and gametocyte proportions during the culturing process (Figure 3 – Figure supplement 1c). The estimates produced from the mixture model approach showed high concordance with those observed by counting Giemsa-stained blood smears (Figure 3 – Figure supplement 1d). Due to the potential confounding effect of differences in stage distribution on gene expression, we adjusted for developmental stage determined by the mixture model in all subsequent analyses.

Our new approach was applied to RNA-sequencing samples of *ex vivo* and short-term *in vitro* cultured parasites from German travellers (Wichers *et al.*, 2021). Table S3 shows the assembled *var* transcripts on a per sample basis. Interestingly, we observed SSPACE did not provide improvement in terms of extending *var* assembled contigs in 9/37 samples. We observed a significant increase in the number of assembled *var* transcripts in generation 2 parasites compared to paired generation 1 parasites ($p_{adj} = 0.04$, paired Wilcoxon test). We observed no significant differences in the length of the assembled *var* transcripts across the generations. Three different filtering approaches were applied in comparison to maximise the likelihood that correct assemblies were taken forward for further analysis and to avoid the overinterpretation of lowly expressed partial *var* transcripts (Table S4). Filtering for *var* transcripts at least 1500nt long and containing at

232 least 3 significantly annotated *var* domains was the least restrictive, while the other approaches required the
233 presence of a DBLα domain within the transcript. All three filtering approaches generated the same maximum
234 length *var* transcript and similar N50 values. This suggests minimal differences in the three filtering
235 approaches, whilst highlighting the importance of filtering assembled *var* transcripts.
236
237 In the original approach of Wichers *et al.*, 2021, the non-core reads of each sample used for *var* assembly
238 were mapped against a pooled reference of assembled *var* transcripts from all samples, as a preliminary step
239 towards differential *var* transcript expression analysis. This approach returned a small number of *var*
240 transcripts which were expressed across multiple patient samples (Figure 3 – Figure supplement 2a). As
241 genome sequencing was not available, it was not possible to know whether there was truly overlap in *var*
242 genomic repertoires of the different patient samples, but substantial overlap was not expected. Stricter
243 mapping approaches (for example, excluding transcripts shorter than 1500nt) changed the resulting *var*
244 expression profiles and produced more realistic scenarios where similar *var* expression profiles were
245 generated across paired samples, whilst there was decreasing overlap across different patient samples (Figure
246 3 – Figure supplement 2b,c). Given this limitation, we used the paired samples to analyse *var* gene expression
247 at an individual subject level, where we confirmed the MSP1 genotypes and alleles were still present after
248 short-term *in vitro* cultivation. The per patient approach showed consistent expression of *var* transcripts
249 within samples from each patient but no overlap of *var* expression profiles across different patients (Figure 3
250 – Figure supplement 2d). Taken together, the per patient approach was better suited for assessing *var*
251 transcriptional changes in longitudinal samples. However, it has been hypothesised that more conserved *var*
252 genes in field isolates increase parasite fitness during chronic infections, necessitating the need to correctly
253 identify them (Dimonte *et al*., 2020, Otto *et al*., 2019). Accordingly, further work is needed to optimise the
254 pooled sample approach to identify truly conserved *var* transcripts across different parasite isolates in cross-
255 sectional studies.
256
257 <u>Longitudinal analysis of *var* transcriptome from *ex vivo* to *in vitro* samples</u>
258 To assess the changes in the *var* transcriptome induced by parasite culturing, we performed a series of
259 analyses, all of which addressed different aspects: (i) changes in individual *var* gene expression pattern and
260 *var* expression homogeneity ("per patient analysis"), (ii) changes in the expression of *var* variants conserved
261 between strains, (iii) changes in the expression of PfEMP1 domains, (iv) changes in expression at the *var* group
262 level, and (v) at the overall *var* expression level. We validated our results using the DBLα-tag approach and
263 complemented the *var* -specific analysis by also examining changes in the core transcriptome.
264
265 To investigate whether dominant *var* gene expression changes through *in vitro* culture, rank analysis of *var*
266 transcript expression was performed (Figure 4, Figure 4 – Figure supplement 1). In most cases a single
267 dominant *var* transcript was detected. The dominant *var* gene did not change in most patient samples and
268 the ranking of *var* gene expression remained similar. However, we observed a change in the dominant *var*
269 gene being expressed through culture in isolates from three of 13 (23%) patients (#6, #17 and #26). Changes
270 in the dominant *var* gene expression were also observed in the DBLα-tag data for these patients (described
271 below). In parasites from three additional patients, #1, #7 and #14, the top expressed *var* gene remained the
272 same, however we observed a change in the ranking of other highly expressed *var* genes in the cultured
273 samples compared to the *ex vivo* sample. Interestingly, in patient #26 we observed a switch from a dominant
274 group A *var* gene to a group B and C *var* gene. This finding was also observed in the DBLα-tag analysis (results
275 below). A similar finding was seen in patient #7. In the *ex vivo* sample, the second most expressed *var*
276 transcript was a group A transcript. However, in the cultured samples expression of this transcript was
277 reduced and we observed an increase in the expression of group B and C *var* transcripts. A similar pattern was
278 observed in the DBLα-tag analysis for patient #7, whereby the expression of a group A transcript was reduced
279 during the first cycle of cultivation. Overall, the data suggest that some patient samples underwent a larger

var transcriptional change when cultured compared to the other patient samples and that culturing parasites can lead to an unpredictable *var* transcriptional change.

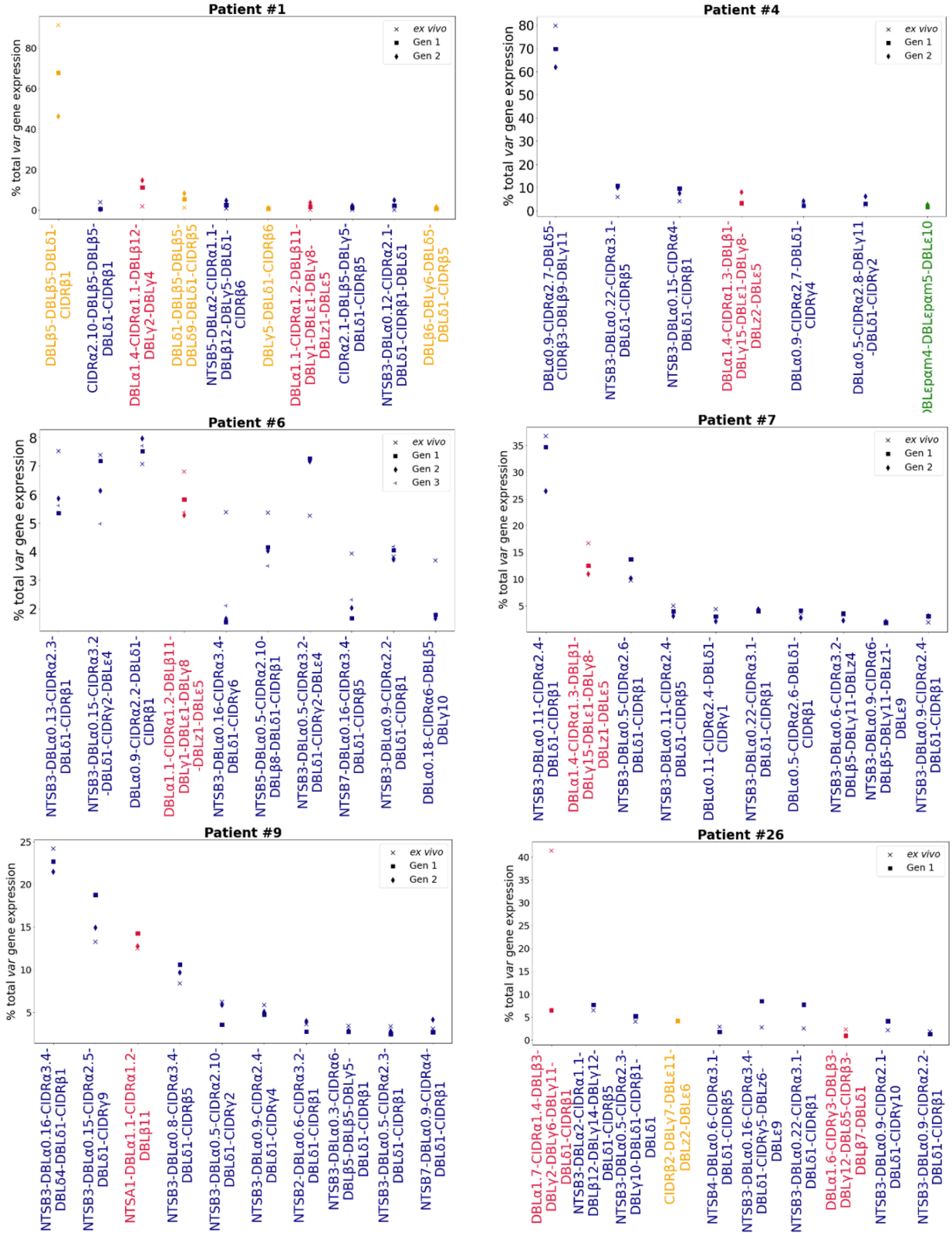

Figure 4: Rank *var* gene expression analysis. For each patient, the paired *ex vivo* (n=13) and *in vitro* samples (generation 1: n=13, generation 2: n=10, generation 3: n=1) were analysed. The assembled *var* transcripts with at least 1500nt and containing 3 significantly annotated *var* domains across all the generations for a patient were combined into a reference, redundancy was removed using cd-hit (at sequence identity = 99%), and expression was quantified using Salmon. *Var* transcript expression was ranked. Plots show the top 10 *var* gene expression rankings for each patient and their *ex vivo* and short-term *in vitro* cultured parasite samples. Group A *var* transcripts (red), group B or C *var* transcripts (blue), group E *var* transcripts (green) and transcripts of unknown *var* group (orange).

282 In line with these results, *var* expression homogeneity (VEH) on a per patient basis showed in some patients
283 a clear change, with the *ex vivo* sample diversity curve distinct from those of *in vitro* generation 1 and
284 generation 2 samples (patients #1, #2, #4) (Figure 4 – Figure supplement 2). Similarly, in other patient samples,
285 we observed a clear difference in the curves of *ex vivo* and generation 1 samples (patient #25 and #26, both
286 from first-time infected severe malaria patients). Some of these samples (#1 and #26, both from first-time
287 infected severe malaria patients) also showed changes in their dominant *var* gene expression during culture,
288 taken together indicating much greater *var* transcriptional changes *in vitro* compared to the other samples.
289
290 Expression of conserved *var* gene variants through short-term *in vitro* culture
291 Due to the relatively high level of conservation observed in *var1, var2csa* and *var3*, they do not present with
292 the same limitations as regular *var* genes. Therefore, changes in their expression through short-term culture
293 was investigated across all samples together. We observed no significant differences in the expression of
294 conserved *var* gene variants, *var1-IT* (p_{adj} = 0.61, paired Wilcoxon test), *var1-3D7* (p_{adj} =0.93, paired Wilcoxon
295 test) and *var2csa* (p_{adj} =0.54, paired Wilcoxon test) between paired *ex vivo* and generation 1 parasites, but
296 *var2csa* was significantly differentially expressed between generation 1 and generation 2 parasites (p_{adj} =
297 0.029, paired Wilcoxon test) (Figure 4 – Figure supplement 3). However, *var2csa* expression previously
298 appeared to have decreased in some paired samples during the first cycle of cultivation (Figure 4 – Figure
299 supplement 3).
300
301 Differential expression of *var* domains from *ex vivo* to *in vitro* samples
302 There is overlap in PfEMP1 domain subtypes of different parasite isolates which can be associated with *var*
303 gene groups and receptor binding phenotypes. This allows performing differential expression analysis on the
304 level of encoded PfEMP1 domain subtypes, as done in previous studies (Tonkin-Hill *et al.*, 2018, Wichers *et*
305 *al.*, 2021). PCA on *var* domain expression (Figure 5a) showed some patients' *ex vivo* samples clustering away
306 from their respective generation 1 sample (patient #1, #2, #4, #12, #17, #25), again indicating a greater *var*
307 transcriptional change relative to the other samples during the first cycle of cultivation. However, in the
308 pooled comparison of the generation 1 vs *ex vivo* of all isolates, a single domain was significantly differentially
309 expressed, CIDRα2.5 associated with B-type PfEMP1 proteins and CD36-binding (Figure 5b). In the generation
310 2 vs *ex vivo* comparison, there were no domains significantly differentially expressed, however we observed
311 large $\log_2$FC values in similar domains to those changing most in the *ex vivo* vs generation 1 comparison (Figure
312 5c). No differentially expressed domains were found in the generation 1 vs generation 2 comparison. These
313 results suggest individual changes in *var* expression are not reflected in the pooled analysis and the per patient
314 approach is more suitable.
315
316 *Var* group expression analysis
317 A previous study found group A *var* genes to have a rapid transcriptional decline in culture compared to group
318 B *var* genes, however another study found a decrease in both group A and group B *var* genes in culture (Zhang
319 *et al.*, 2011, Peters *et al.*, 2007). These studies were limited as the *var* type was determined by analysing the
320 sequence diversity of DBLα domains, and by quantitative PCR (qPCR) methodology which restricts analysis to
321 quantification of known/conserved sequences. Due to these results, the expression of group A *var* genes vs.
322 group B and C *var* genes was investigated using a paired analysis on all the DBLα (DBLα1 vs DBLα0 and DBLα2)
323 and NTS (NTSA vs NTSB) sequences assembled from *ex vivo* samples and across multiple generations in
324 culture. A linear model was created with group A expression as the response variable, the generation and life
325 cycle stage as independent variables and the patient information included as a random effect. The same was
326 performed using group B and C expression levels.

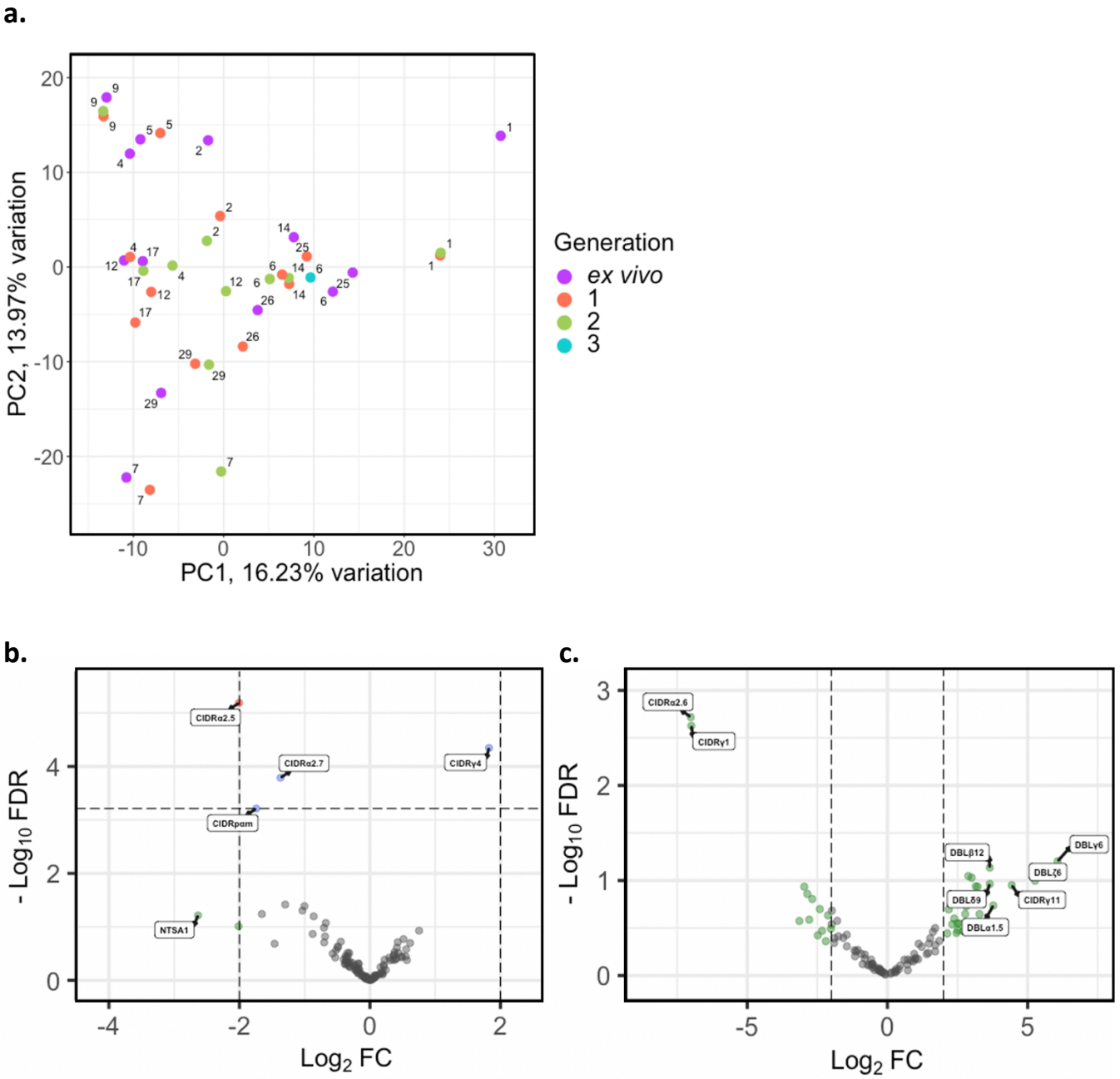

Figure 5: *Var* domain transcriptome analysis through short-term *in vitro* culture. *Var* transcripts for paired *ex vivo* (n=13), generation 1 (n=13), generation 2 (n=10) and generation 3 (n=1) were *de novo* assembled using the whole transcript approach. *Var* transcripts were filtered for those >= 1500nt in length and containing at least 3 significantly annotated *var* domains. Transcripts were annotated using HMM models built on the Rask et al., 2010 dataset (Rask *et al.*, 2010). When annotating the whole transcript, the most significant alignment was taken as the best annotation for each region of the assembled transcript (e-value cut off 1e-5). Multiple annotations were allowed on the transcript if they were not overlapping, determined using cath-resolve-hits. *Var* domain expression was quantified using FeatureCounts and the domain counts aggregated **a)** PCA plot of $\log_2$ normalized read counts (adjusted for life cycle stage, derived from the mixture model approach). Points are coloured by their generation (*ex vivo*; purple, generation 1; red, generation 2; green and generation 3; blue) and labelled by their patient identity **b)** Volcano plot showing extent and significance of up- or down-regulation of *var* domain expression in *ex vivo* (n=13) compared with paired generation 1 cultured parasites (n=13) (red and blue, $P < 0.05$ after Benjamini-Hochberg adjustment for FDR; red and green, absolute $\log_2$ fold change $\log_2$FC in expression >= 2). Domains with a $\log_2$FC > = 2 represent those upregulated in generation 1 parasites. Domains with a $\log_2$FC <= -2 represent those downregulated in generation 1 parasites. **c)** Volcano plot showing extent and significance of up- or down-regulation of *var* domain expression in *ex vivo* (n=10) compared with paired generation 2 cultured parasites (n=10) (green, absolute $\log_2$ fold change $\log_2$FC in expression >= 2). Domains with a $\log_2$FC >= 2 represent those upregulated in generation 2 parasites. Domains with a $\log_2$FC <= -2 represent those downregulated in generation 2 parasites. Differential expression analysis was performed using DESeq2 (adjusted for life cycle stage, derived from the mixture model approach).

327

In both approaches, DBLα and NTS, we found no significant changes in total group A or group B and C *var* gene expression levels (Figure 6). We observed high levels of group B and C *var* gene expression compared to group A in all patients, both in the *ex vivo* samples and the *in vitro* samples. In some patients we observed a decrease in group A *var* genes from *ex vivo* to generation 1 (patients #1, #2, #5, #6, #9, #12, #17, #26) (Figure 6a), however in all but four patients (patient #1, #2, #5, #6) the levels of group B and C *var* genes remained consistently high from *ex vivo* to generation 1 (Figure 6b). Interestingly, patients #6 and #17 also had a change in the dominant *var* gene expression through culture. Taken together with the preceding results, it appears that observed differences in *var* transcript expression occurring with transition to short-term culture are not due to modulation of recognised *var* classes, but due to differences in expression of particular *var* transcripts.

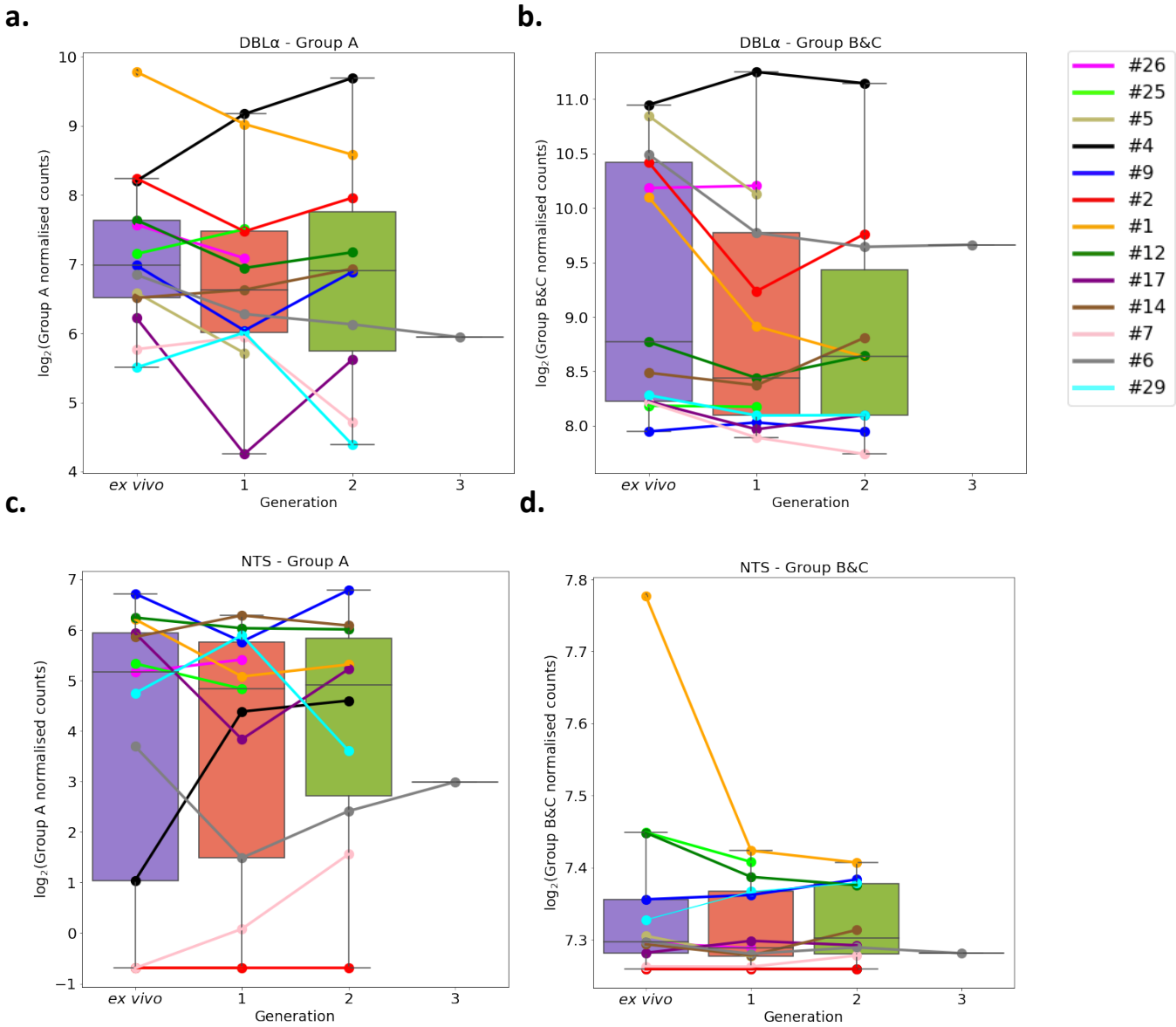

Figure 6. *Var* group expression analysis through short-term *in vitro* culture. The DBLα domain sequence for each transcript was determined and for each patient a reference of all assembled DBLα domains combined. Group A *var* genes possess DBLα1 domains, some group B encode DBLα2 domains and groups B and C encode DBLα0 domains. Domains were grouped by type and their expression summed. The relevant sample's non-core reads were mapped to this using Salmon and DBLα expression quantified. DESeq2 normalisation was performed, with patient identity and life cycle stage proportions included as covariates. A similar approach was repeated for NTS domains. Group A *var* genes encode NTSA compared to group B and C *var* genes which encode NTSB. Boxplots show $\log_2$ normalised Salmon read counts for **a)** group A *var* gene expression through cultured generations assessed using the DBLα domain sequences, **b)** group B and C *var* gene expression through cultured generations assessed using the DBLα domain sequences, **c)** group A *var* gene expression through cultured generations assessed using the NTS domain sequences, and **d)** group B and C *var* gene expression through cultured generations assessed using the NTS domain sequences. Different coloured lines connect paired patient samples through the generations: *ex vivo* (n=13), generation 1 (n=13), generation 2 (n=10) and generation 3 (n=1). Axis shows different scaling.

337
338 Quantification of total *var* gene expression
339 We observed a trend of decreasing total *var* gene expression between generations irrespective of the
340 assembler used in the analysis (Figure 6 – Figure supplement 1). A similar trend is seen with the LARSFADIG
341 count, which is commonly used as a proxy for the number of different *var* genes expressed (Otto *et al.*, 2019).
342 A linear model was created (using only paired samples from *ex vivo* and generation 1) (Supplementary file 1)
343 with proportion of total gene expression dedicated to *var* gene expression as the response variable, the
344 generation and life cycle stage as independent variables and the patient information included as a random
345 effect. This model showed no significant differences between generations, suggesting that differences
346 observed in the raw data may be a consequence of small changes in developmental stage distribution in
347 culture.
348
349 Validation of *var* expression profiling by DBLα-tag sequencing
350 Deep sequencing of RT-PCR-amplified DBLα expressed sequence tags (ESTs) combined with prediction of the
351 associated transcripts and their encoded domains using the Varia tool (Mackenzie *et al.*, 2022) was performed
352 to supplement the RNA-sequencing analysis. The raw Varia output file is given in Supplementary file 2. Overall,
353 we found a high agreement between the detected DBLα-tag sequences and the *de novo* assembled *var*
354 transcripts. A median of 96% (IQR: 93–100%) of all unique DBLα-tag sequences detected with >10 reads were
355 found in the RNA-sequencing approach. This is a significant improvement on the original approach (p= 0.0077,
356 paired Wilcoxon test), in which a median of 83% (IQR: 79–96%) was found (Wichers *et al.*, 2021). To allow for
357 a fair comparison of the >10 reads threshold used in the DBLα-tag approach, the upper 75th percentile of the
358 RNA-sequencing-assembled DBLα domains were analysed. A median of 77.4% (IQR: 61–88%) of the upper
359 75th percentile of the assembled DBLα domains were found in the DBLα-tag approach. This is a lower median
360 percentage than the median of 81.3% (IQR: 73–98%) found in the original analysis (p= 0.28, paired Wilcoxon
361 test) and suggests the new assembly approach is better at capturing all expressed DBLα domains.
362
363 The new whole transcript assembly approach also had high consistency with the domain annotations
364 predicted from Varia. Varia predicts *var* sequences and domain annotations based on short sequence tags,
365 using a database of previously defined *var* sequences and annotations (Mackenzie *et al.*, 2022). A median of
366 85% of the DBLα annotations and 73% of the DBLα-CIDR domain annotations, respectively, identified using
367 the DBLα-tag approach were found in the RNA sequencing approach. This further confirms the performance
368 of the whole transcript approach and it was not restricted by the pooled approach of the original analysis. We
369 also observed consistent results with the per patient analysis, in terms of changes in the dominant *var* gene
370 expression (described above) (Supplementary file 2). In line with the RNA-sequencing data, the DBLα-tag
371 approach revealed no significant differences in Group A and Group B and C groups during short-term culture,
372 further highlighting the agreement of both methods (Figure 6 – Figure supplement 2).
373
374 Differential expression analysis of the core transcriptome between *ex vivo* and *in vitro* samples
375 Given the modest changes in *var* gene expression repertoire upon culture we wanted to investigate the extent
376 of any accompanying changes in the core parasite transcriptome. PCA was performed on core gene (*var, rif,*
377 *stevor, surf* and rRNA genes removed) expression, adjusted for life cycle stage. We observed distinct clustering
378 of *ex vivo*, generation 1, and generation 2 samples, with patient identity having much less influence (Figure
379 7a). There was also a change from the heterogeneity between the *ex vivo* samples to more uniform clustering
380 of the generation 1 samples (Figure 7a), suggesting that during the first cycle of cultivation the core
381 transcriptomes of different parasite isolates become more alike.

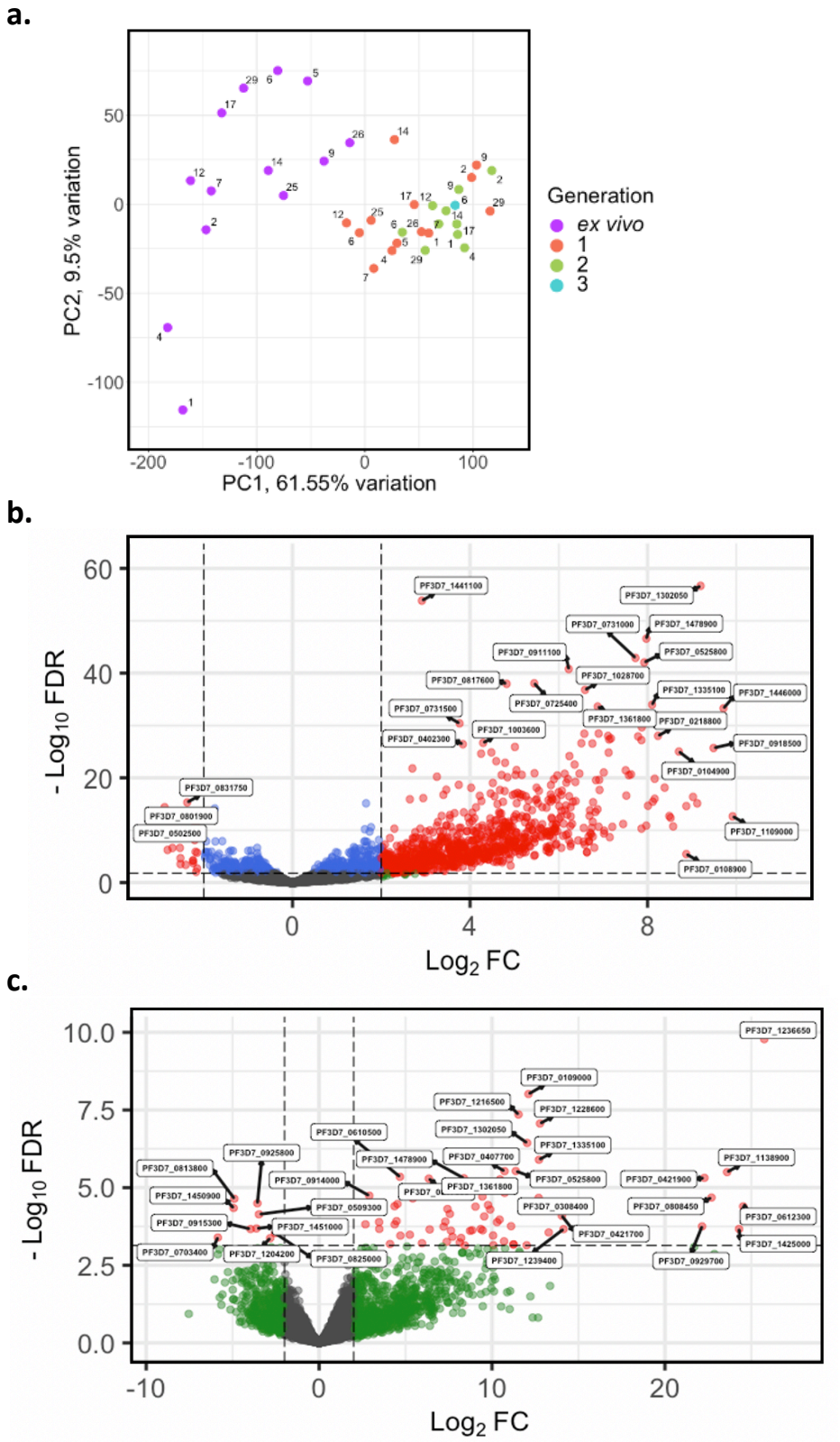

Figure 7: Core gene transcriptome analysis of *ex vivo* and short-term *in vitro* cultured samples. Core gene expression was assessed for paired *ex vivo* (n=13), generation 1 (n=13), generation 2 (n=10) and generation 3 (n=1) parasite samples. Subread align was used, as in the original analysis, to align the reads to the human genome and *P. falciparum* 3D7 genome, *with var, rif, stevor, surf* and *rRNA* genes removed. HTSeq count was used to quantify gene counts. **a)** PCA plot of $\log_2$ normalized read counts. Points are coloured by their generation (*ex vivo*: purple, generation 1: red, generation 2: green, and generation 3: blue) and labelled by their patient identity. **b)** Volcano plot showing extent and significance of up- or down-regulation of core gene expression in *ex vivo* (n=13) compared with paired generation 1 cultured parasites (n=13) and **c)** in *ex vivo* (n=10) compared with paired generation 2 cultured parasites (n=10). Dots in red and blue represent those genes with $P < 0.05$ after Benjamini-Hochberg adjustment for FDR, red and green dots label genes with absolute $\log_2$ fold change $\log_2$FC in expression >= 2). Accordingly, genes with a $\log_2$FC > = 2 represent those upregulated in generation 1 parasites and genes with a $\log_2$FC <= -2 represent those downregulated in generation 1 parasites. Normalized read counts of the core gene analysis were adjusted for life cycle stage, derived from the mixture model approach.

382

In total, 920 core genes (19% of the core transcriptome) were found to be differentially expressed after adjusting for life cycle stages using the mixture model approach between *ex vivo and* generation 1 samples (Supplementary file 3). The majority were upregulated, indicating a substantial transcriptional change during the first cycle of *in vitro* cultivation (Figure 7b). 74 genes were found to be upregulated in generation 2 when compared to the *ex vivo* samples, many with $\log_2$FC greater than those in the *ex vivo* vs generation 1 comparison (Figure 7c). No genes were found to be significantly differentially expressed between generation 1 and generation 2. However, five genes had a $\log_2$FC >= 2 and were all upregulated in generation 2 compared to generation 1. Interestingly, the gene with the greatest fold change, encoding ROM3 (PF3D7_0828000), was also found to be significantly downregulated in generation 1 parasites in the *ex vivo* vs generation 1 analysis. The other four genes were also found to be non-significantly downregulated in generation 1 parasites in the *ex vivo* vs generation 1 analysis. This suggests changes in gene expression during the first cycle of cultivation are the greatest compared to the other cycles.

The most significantly upregulated genes (in terms of fold change) in generation 1 contained several small nuclear RNAs, splicesomal RNAs and non-coding RNAs (ncRNAs). 16 ncRNAs were found upregulated in generation 1, with several RNA-associated proteins having large fold changes ($\log_2$FC > 7) Significant gene ontology (GO) terms and Kyoto encyclopedia of genes and genomes (KEGG) pathways for the core genes upregulated in generation 1 included "entry into host", "movement into host" and "cytoskeletal organisation" suggesting the parasites undergo a change in invasion efficiency, which is connected to the cytoskeleton, during their first cycle of *in vitro* cultivation (Figure 7 – Figure supplement 1). We observed eight AP2 transcription factors upregulated in generation 1 (PF3D7_0404100/AP2-SP2, PF3D7_0604100/SIP2, PF3D7_0611200/AP2-EXP2, PF3D7_0613800, PF3D7_0802100/AP2-LT, PF3D7_1143100/AP2-O, PF3D7_1239200, PF3D7_1456000/AP2-HC) with no AP2 transcription factors found to be downregulated in generation 1. To confirm the core gene expression changes identified were not due to the increase in parasite age during culture, as indicated by upregulation of many schizont-related genes, core gene differential expression analysis was performed on paired *ex vivo* and generation 1 samples that contained no schizonts or gametocytes in generation 1. The same genes were identified as significantly differentially expressed with a Spearman's rank correlation of 0.99 for the $\log_2$FC correlation between this restricted sample approach and those produced using all samples (Figure 7 – Figure supplement 2).

<u>Cultured parasites as surrogates for assessing the *in vivo* core gene transcriptome</u>

In the original analysis of *ex vivo samples*, hundreds of core genes were identified as significantly differentially expressed between pre-exposed and naïve malaria patients. We investigated whether these differences persisted after *in vitro* cultivation. We performed differential expression analysis comparing parasite isolates from naïve (n=6) vs pre-exposed (n=7) patients, first between their *ex vivo* samples, and then between the corresponding generation 1 samples. Interestingly, when using the *ex vivo* samples, we observed 206 core genes significantly upregulated in naïve patients compared to pre-exposed patients (Figure 7 – Figure supplement 3a). Conversely, we observed no differentially expressed genes in the naïve vs pre-exposed analysis of the paired generation 1 samples (Figure 7 – Figure supplement 3b). Taken together with the preceding findings, this suggests one cycle of cultivation shifts the core transcriptomes of parasites to be more alike each other, diminishing inferences about parasite biology *in vivo*.

Table 3 provides an overview of the different levels of analysis performed, including their rationale, the methods used, the resulting findings, and their interpretation.

Table 3: Summary of the different levels of analysis performed to assess the effect of short-term parasite culturing on *var* and core gene expression, their rational, method, results, and interpretation.

Analysis level	Analysis	Rationale	Method	Results	Interpretation
***var* transcript**	Per patient expression ranking	Relative quantification of *var* transcripts over consecutive generations of parasites originating from the same patient to reveal *var* gene switching events	Combine assembled *var* transcripts for each patient into a reference and quantify expression, validated with DBLα-tag analysis	46% of the patient samples had a change in the dominant or top 3 highest expressed *var* gene	Modest changes in most samples, but unpredictable *var* gene switching during culture in some samples
	Per patient *var* expression homogeneity (VEH)	Determine the overall diversity of *var* gene expression (number of different variants expressed and their abundance) to assess impact of culturing on the overall *var* gene expression pattern	Comparison of diversity curves based on per patient quantification of the *var* transcriptome	39% of *ex vivo* samples diversity curves distinct from *in vitro* samples	Some patient samples underwent a much greater *var* transcriptional change compared to others
	Conserved *var* variants	Assessing and comparing the expression levels of strain-transcendent *var* gene variants (*var1*, *var2csa*, *var3*) between samples	Reference of all assembled transcripts for each conserved *var* gene and quantify expression	*var2csa* expression increases in 2nd *in vitro* generation	Parasites converge to *var2csa* during short-term *in vitro* culture
***var*-encoded PfEMP1 domains**	Differential expression of PfEMP1 domains	Identification, quantification and comparison of expression levels of different *var* gene-encoded PfEMP1 domains associated with different disease manifestations	Pool all assembled *var* transcripts into a reference and quantify expression of each domain	46% of the *ex vivo* samples cluster away from their *in vitro* samples in PCA plots, distinct clustering by *in vitro* generation was not observed; CIDRα2.5 significantly differentially expressed between *ex vivo* and generation 1	Transition to culture results in modest modulation of particular *var* domains
***var* group**	Expression of NTS (NTSA vs NTSB) and DBLα (DBLα1 vs DBLα0+ DBLα2)	Quantification and comparison of expression levels of different *var* gene groups (group A vs. group B and C)	Create a reference of all assembled DBLα and NTS domains for each patient and quantify expression. Validated with DBLα-tag analysis	No significant changes	No preferential up or down regulation of certain *var* groups during transition to culture
Global *var* expression	LARSFADIG coverage	Assessing the overall *var* gene expression level (excluding *var2csa*)	Assemble the LARSFADIG motif and map non-core reads to quantify coverage	Trend for decrease in global *var* expression during culture, but no significant changes	Subtle reduction in global *var* gene expression may reflect increase in parasite age during culture
Core genes	Differential gene expression (DGE)	Assessing the impact of cultivation on the parasite core gene transcriptome	Differential expression analysis of core genes (*P. falciparum* 3D7 used as reference)	19% of the core transcriptome significantly differentially expressed between paired *ex vivo* and generation 1 *in vitro* samples; distinct clustering by parasite generation observed; upregulation of invasion and replication related genes *in vitro*	Parasites core gene expression changes substantially upon entering culture

Discussion

Multiple lines of evidence point to PfEMP1 as a major determinant of malaria pathogenesis, but previous approaches for characterising *var* expression profiles in field samples have limited *in vivo* studies of PfEMP1 function, regulation, and association with clinical symptoms (Tarr *et al.*, 2018, Lee *et al.*, 2018, Warimwe *et al.*, 2013, Rorick *et al.*, 2013, Zhang *et al.*, 2011, Taylor *et al.*, 2002). A more recent approach, based on RNA-sequencing, overcame many of the limitations imposed by the previous primer-based methods (Tonkin-Hill *et al.*, 2018, Wichers *et al.*, 2021). However, depending on the expression level and sequencing depth, *var* transcripts were found to be fragmented and only a partial reconstruction of the *var* transcriptome was achieved (Tonkin-Hill *et al.*, 2018, Wichers *et al.*, 2021, Andrade *et al.*, 2020, Guillochon *et al.*, 2022, Yamagishi *et al.*, 2014). The present study developed a novel approach for *var* gene assembly and quantification that overcomes many of these limitations.

Our new approach used the most geographically diverse reference of *var* gene sequences to date, which improved the identification of reads derived from *var* transcripts. This is crucial when analysing patient samples with low parasitaemia where *var* transcripts are hard to assemble due to their low abundancy (Guillochon *et al.*, 2022). Our approach has wide utility due to stable performance on both laboratory-adapted and clinical samples. Concordance in the different *var* expression profiling approaches (RNA-sequencing and DBLα-tag) on *ex vivo* samples increased using the new approach by 13%, when compared to the original approach (96% in the whole transcript approach compared to 83% in Wichers *et al.*, 2021. This suggests the new approach provides a more accurate method for characterising *var* genes, especially in samples collected directly from patients. Ultimately, this will allow a deeper understanding of relationships between *var* gene expression and clinical manifestations of malaria.

Having a low number of long contigs is desirable in any *de novo* assembly. This reflects a continuous assembly, as opposed to a highly fragmented one where polymorphic and repeat regions could not be resolved (Lischer & Shimizu, 2017). An excessive number of contigs cannot be reasonably handled computationally and results

from a high level of ambiguity in the assembly (Yang *et al.*, 2012). We observed a greater than 50% reduction in the number of contigs produced in our new approach, which also had a 21% increase in the maximum length of the assembled *var* transcripts, when compared to the original approach. It doubled the assembly continuity and assembled an average of 13% more of the *var* transcripts. This was particularly apparent in the N-terminal region, which has often been poorly characterised by existing approaches. The original approach failed to assemble the N-terminal region in 58% of the samples, compared to just 4% in the new approach with assembly consistently achieved with an accuracy > 90%. This is important because the N-terminal region is known to contribute to the adhesion phenotypes of most PfEMP1 proteins.

The new approach allows for *var* transcript reconstruction across a range of expression levels, which is required when characterising *var* transcripts from multi-clonal infections. Assembly completeness of the lowly expressed *var* genes increased five-fold using the new approach. Biases towards certain parasite stages have been observed in non-severe and severe malaria cases, so it is valuable to assemble the *var* transcripts from different life cycle stages (Tonkin-Hill *et al.*, 2018). Our new approach is not limited by parasite stage. It was able to assemble the whole *var* transcript, in a single contig, at later stages in the *P. falciparum* 3D7 intra-erythrocytic cycle, something previously unachievable. The new approach allows for a more accurate and complete picture of the *var* transcriptome. It provides new perspectives for relating *var* expression to regulation, co-expression, epigenetics and malaria pathogenesis. It can be applied for example in analysis of patient samples with different clinical outcomes and longitudinal tracking of infections *in vivo*. It represents a crucial improvement for quantifying the *var* transcriptome. In this work, the improved approach for *var* gene assembly and quantification was used to characterise *var* gene expression during transition from *in vivo* to short-term culture.

This study had substantial power through the use of paired samples. However, many *var* gene expression studies do not have longitudinal sampling. Future work should focus on identifying the best approach for analysing the *var* transcripts in cross-sectional samples. Higher level *var* classification systems, such as the PfEMP1 predicted binding phenotype or domain cassettes, could be applied to test for over-representation of different *var* gene features in different groups of interest, because the assumption of overlapping *var* repertoires at these levels of classification would be more realistic. This was briefly explored in our analysis through *var* domain differential expression analysis, which found minimal changes in *var* domain expression through short-term culture, supporting the per patient analysis results. This could be further improved by advancing the classifications of domain subtypes. This has recently been studied using MEME to identify short nucleotide motifs that are representative of domain subtypes (Otto et al., 2019). Other research could investigate clustering *var* transcripts based on sequence identity and testing for clusters associated with specific malaria disease groups.

Studies have been performed investigating differences between long-term laboratory-adapted clones and clinical isolates, with hundreds of genes found to be differentially expressed (Hoo *et al.*, 2019, Tarr *et al.*, 2018, Mackinnon *et al.*, 2009). Surprisingly, studies investigating the impact of short-term culture on parasites are extremely limited, despite it being commonly undertaken for making inferences about the *in vivo* transcriptome (Vignali *et al.*, 2011). Using the new *var* assembly approach, we found that *var* gene expression remains relatively stable during transition to culture. However, the conserved *var2csa* had increased expression from generation 1 to generation 2. It has previously been suggested that long-term cultured parasites converge to expressing *var2csa*, but our findings suggest this begins within two cycles of cultivation (Zhang *et al.*, 2022, Mok *et al.*, 2008). Switching to *var2csa* has been shown to be favourable and is suggested to be the default *var* gene upon perturbation to *var* specific heterochromatin (Ukaegbu *et al.*, 2015). These studies also suggested *var2csa* has a unique role in *var* gene switching and our results are consistent with the role of *var2csa* as the dominant "sink node" (Zhang *et al.*, 2022, Ukaegbu *et al.*, 2015, Ukaegbu *et al.*, 2014, Mok *et al.*, 2008). A previous study suggested *in vitro* cultivation of controlled human malaria infection samples resulted in dramatic changes in *var* gene expression (Lavstsen *et al.*, 2005, Peters *et al.*, 2007). Almost

506 a quarter of samples in our analysis showed more pronounced and unpredictable changes. In these
507 individuals, the dominant *var* gene being expressed changed within one cycle of cultivation. This implies short-
508 term culture can result in unpredictable *var* gene expression as observed previously using a semi-quantitative
509 RT-PCR approach (Bachmann *et al.*, 2011) and that one would need to confirm *in vivo* expression matches *in*
510 *vitro* expression. This can be achieved using the assembly approach described here.
511
512 We observed no generalised pattern of up- or downregulation of specific *var* groups following transition to
513 culture. This implies there is probably not a selection event occurring during culture but may represent a loss
514 of selection that is present *in vivo.* A global down regulation of certain *var* groups might only occur as a
515 selective process over many cycles in extended culture. Determining changes in *var* group expression levels
516 are difficult using degenerate qPCR primers bias and previous studies have found conflicting results in terms
517 of changes of expression of *var* groups through cultivation. Zhang *et al.*, 2011 found a rapid transcriptional
518 decline of group A and group B *var* genes, however Peters *et al.*, 2007 found group A *var* genes to have a high
519 rate of downregulation, when compared to group B *var* genes. These studies differed in the stage distribution
520 of the parasites and were limited in measuring enough variants through their use of primers. Our new
521 approach allowed for the identification of more sequences, with 26.6% of assembled DBLα domains not found
522 via the DBLα-tag approach. This better coverage of the expressed *var* diversity was not possible in these
523 previous studies and may explain discrepancies observed.
524
525 Generally, there was a high consensus between all levels of *var* gene analysis and changes observed during
526 short-term *in vitro* cultivation. However, the impact of short-term culture was the most apparent at the *var*
527 transcript level and became less clear at the *var* domain, *var* type and global *var* gene expression level. This
528 highlights the need for accurate characterisation of full length *var* transcripts and analysis of the *var*
529 transcriptome at different levels, both of which can be achieved with the new approach developed here.
530
531 We saw striking changes in the core gene transcriptomes between *ex vivo* and generation 1 parasites with
532 19% of the core genome being differentially expressed. A previous study showed that expression of 18% of
533 core genes were significantly altered after ~50 cycles through culture (Mackinnon *et al.*, 2009), but our data
534 suggest that much of this change occurs early in the transition to culture. We observed genes with functions
535 unrelated to ring-stage parasites were among those most significantly expressed in the generation 1 vs *ex vivo*
536 analysis, suggesting the culture conditions may temporarily dysregulate stage-specific expression patterns or
537 result in the parasites undergoing a rapid adaptation response (Andreadaki *et al.*, 2020, Beeson *et al.*, 2016).
538 Several AP2 transcription factors (AP2-SP2, AP2-EXP2, AP2-LT, AP2-O and AP2-HC) were upregulated in
539 generation 1. AP2-HC has been shown to be expressed in asexual parasites (Carrington *et al.*, 2021). AP2-O is
540 thought to be specific for the ookinete stage and AP2-SP2 plays a key role in sporozoite stage specific gene
541 expression (Kaneko *et al.*, 2015, Yuda *et al.*, 2010). Our findings are consistent with another study investigating
542 the impact of long-term culture (Mackinnon *et al.*, 2009) which also found genes like merozoite surface
543 proteins differentially expressed, however they were downregulated in long-term cultured parasites, whereas
544 we found them upregulated in generation 1. This suggests short-term cultured parasites might be
545 transcriptionally different from long-term cultured parasites, especially in their invasion capabilities,
546 something previously unobserved. Several genes involved in the stress response of parasites were
547 upregulated in generation 1, for example DnaJ proteins, serine proteases and ATP dependent CLP proteases
548 (Oakley *et al.*, 2007). The similarity of the core transcriptomes of the *in vitro* samples compared to the
549 heterogeneity seen in the *ex vivo* samples could be explained by a stress response upon entry to culture.
550 Studies investigating whether the dysregulation of stage specific expression and the expression of stress
551 associated genes persist in long-term culture are required to understand whether they are important for
552 growth in culture. Critically, the marked differences presented here suggest the impact of short-term culture
553 can override differences observed in both the *in vivo* core and *var* transcriptomes of different disease
554 manifestations.

555 In summary, we present an enhanced approach for *var* transcript assembly which allows for *var* gene
556 expression to be studied in connection to *P. falciparum's* core transcriptome through RNA-sequencing. This
557 will be useful for expanding our understanding of *var* gene regulation and function in *in vivo* samples. As an
558 example of the capabilities of the new approach, the method was used to quantify differences in gene
559 expression upon short-term culture adaptation. This revealed that inferences from clinical isolates of *P.*
560 *falciparum* put into short-term culture must be made with a degree of caution. Whilst *var* gene expression is
561 often maintained, unpredictable switching does occur, necessitating that the similarity of *in vivo* and *in vitro*
562 expression should be confirmed. The more extreme changes in the core transcriptome could have much
563 bigger implications for understanding other aspects of parasite biology such as growth rates and drug
564 susceptibility and raise a need for additional caution. Further work is needed to examine *var* and core
565 transcriptome changes during longer term culture on a larger sample size. Understanding the ground truth of
566 the *var* expression repertoire of *Plasmodium* field isolates still presents a unique challenge and this work
567 expands the database of *var* sequences globally. The increase in long-read sequencing and the growing size
568 of *var* gene databases containing isolates from across the globe will help overcome this issue in future studies.
569

570 ## Materials and Methods

571

572 ### Ethics statement

573 The study was conducted according to the principles of the Declaration of Helsinki, 6th edition, and the
574 International Conference on Harmonization-Good Clinical Practice (ICH-GCP) guidelines. All 32 patients were
575 treated as inpatients or outpatients in Hamburg, Germany (outpatient clinic of the University Medical Center
576 Hamburg-Eppendorf (UKE) at the Bernhard Nocht Institute for Tropical Medicine, UKE,
577 Bundeswehrkrankenhaus) (Wichers *et al.*, 2021). Blood samples for this analysis were collected after patients
578 had been informed about the aims and risks of the study and had signed an informed consent form for
579 voluntary blood collection (n=21). In the remaining cases, no intended blood samples were collected but
580 residuals from diagnostic blood samples were used (n=11). The study was approved by the responsible ethics
581 committee (Ethics Committee of the Hamburg Medical Association, reference numbers PV3828 and PV4539).
582

583 ### Blood sampling, processing and *in vitro* cultivation of *P. falciparum*

584 EDTA blood samples (1–30 mL) were collected from 32 adult falciparum malaria patients for *ex vivo*
585 transcriptome profiling as reported by Wichers *et al.*, 2021 (Wichers *et al.*, 2021), hereafter termed "the
586 original analysis". Blood was drawn and either immediately processed (#1, #2, #3, #4, #11, #12, #14, #17, #21,
587 #23, #28, #29, #30, #31, #32) or stored overnight at 4°C until processing (#5, #6, #7, #9, #10, #13, #15, #16,
588 #18, #19, #20, #22, #24, #25, #26, #27, #33). If samples were stored overnight, the *ex vivo* and *in vitro* samples
589 were still processed at the same time (so paired samples had similar storage). Erythrocytes were isolated by
590 Ficoll gradient centrifugation, followed by filtration through Plasmodipur filters (EuroProxima) to remove
591 residual granulocytes. At least 400 µl of the purified erythrocytes were quickly lysed in 5 volumes of pre-
592 warmed TRIzol (ThermoFisher Scientific) and stored at -80°C until further processing ("*ex vivo* samples").
593 When available, the remainder was then transferred to *in vitro* culture either without the addition of
594 allogeneic red cells or with the addition of O+ human red cells (blood bank, UKE) for dilution according to a
595 protocol adopted from Trager and Jensen (Table S5). Cultures were maintained at 37°C in an atmosphere of
596 1% O2, 5% CO2, and 94% N2 using RPMI complete medium containing 10% heat-inactivated human serum
597 (A+, Interstate Blood Bank, Inc., Memphis, USA). Cultures were sampled for RNA purification at the ring stage
598 by microscopic observation of the individual growth of parasite isolates, and harvesting was performed at the
599 appropriate time without prior synchronization treatment ("*in vitro* samples"). 13 of these *ex vivo* samples
600 underwent one cycle of *in vitro* cultivation, ten of these generation 1 samples underwent a second cycle of *in*
601 *vitro* cultivation. One of these generation 2 samples underwent a third cycle of *in vitro* cultivation (Table 1).
602 In addition, an aliquot of *ex vivo* erythrocytes (approximately 50–100 µl) and aliquots of *in vitro* cell cultures

603 collected as indicated in Supplementary file 4 were processed for gDNA purification and MSP1 genotyping as
604 described elsewhere (Wichers *et al.*, 2021, Robert *et al.*, 1996).
605
606 RNA purification, RNA-sequencing library preparation, and sequencing
607 RNA purification was performed as described in Wichers *et al.*, 2021, using TRIzol in combination with the
608 RNeasy MinElute Kit (Qiagen) and DNase digestion (DNase I, Qiagen). Human globin mRNA was depleted from
609 all samples except from samples #1 and #2 using the GLOBINclear kit (ThermoFisher Scientific). The median
610 RIN value over all *ex vivo* samples was 6.75 (IQR: 5.93–7.40), although this measurement has only limited
611 significance for samples containing RNA of two species. Accordingly, the RIN value increased upon cultivation
612 for all *in vitro* samples (Supplementary file 5). Customized library construction in accordance to Tonkin-Hill *et*
613 *al.,* 2018, including amplification with KAPA polymerase and HiSeq 2500 125 bp paired-end sequencing was
614 performed by BGI Genomics Co. (Hong Kong).
615
616 Methods for assembling *var* genes
617 Previously Oases, Velvet, SoapDeNovo-Trans or MaSuRCA have been used for *var* transcript assembly
618 (Wichers *et al.*, 2021, Andrade *et al.*, 2020, Otto *et al.*, 2019, Tonkin-Hill *et al.*, 2018). Previous methods either
619 did not incorporate read error correction or focussed on gene assembly, as opposed to transcript assembly
620 (Schulz *et al.*, 2012, Zerbino & Birney, 2008, Xie *et al.*, 2014, Zimin *et al.*, 2013). Read error correction is
621 important for *var* transcript assembly due to the highly repetitive nature of the *P. falciparum* genome. Recent
622 methods have also focused on whole transcript assembly, as opposed to initial separate domain assembly
623 followed by transcript assembly (Wichers *et al.*, 2021, Andrade *et al.*, 2020, Otto *et al.*, 2019, Tonkin-Hill *et*
624 *al.*, 2018). The original analysis used SoapDeNovo-Trans to assemble the *var* transcripts, however it is
625 currently not possible to run all steps in the original approach, due to certain tools being improved and
626 updated. Therefore, SoapDeNovo-Trans (k=71) was used and termed the original approach.
627
628 Here, two novel methods for whole *var* transcript and *var* domain assembly were developed and their
629 performance was evaluated in comparison to the original approach (Figure 2b). In both methods the reads
630 were first mapped to the human g38 genome and any mapped reads were removed. Next, the unmapped
631 reads were mapped to a modified *P. falciparum* 3D7 genome with *var* genes removed, to identify multi-
632 mapping reads commonly present in *Plasmodium* RNA-sequencing datasets. Any mapped reads were
633 removed. In parallel, the unmapped RNA reads from the human mapping stage were mapped against a
634 reference of field isolate *var* exon 1 sequences and the mapped reads identified (Otto *et al.*, 2019). These
635 reads were combined with the unmapped reads from the 3D7 genome mapping stage and duplicate reads
636 removed. All mapping was performed using sub-read align as in the original analysis (Wichers *et al.*, 2021).
637 The reads identified at the end of this process are referred to as "non-core reads".
638
639 Whole *var* transcript and *var* domain assembly methods
640 For whole *var* transcript assembly the non-core reads, for each sample separately, were assembled using
641 rnaSPAdes (k-mer =71, read_error_correction on) (Bushmanova *et al.*, 2019). Contigs were joined into larger
642 scaffolds using SSPACE (parameters -n 31 -x 0 -k 10) (Boetzer *et al.*, 2011). Transcripts < 500nt were excluded,
643 as in the original approach. The included transcripts were annotated using hidden Markov models (HMM)
644 (Finn *et al.*, 2011) built on the *Rask et al.*, 2010 dataset and used in Tonkin-Hill *et al.*, 2018. When annotating
645 the whole transcript, the most significant alignment was taken as the best annotation for each region of the
646 assembled transcript (e-value cut off 1e-5). Multiple annotations were allowed on the transcript if they were
647 not overlapping, determined using cath-resolve-hits (Lewis *et al.*, 2019). Scripts are available in the GitHub
648 repository (https://github.com/ClareAndradiBrown/varAssembly)
649
650 In the *var* domain assembly approach, separate domains were assembled first and then joined up to form
651 transcripts. First, the non-core reads were mapped (nucleotide basic local alignment tool (blastn) short read

652 option) to the domain sequences as defined in Rask *et al.*, 2010. This was found to produce similar results
653 when compared to using tblastx. An e-value threshold of 1e-30 was used for the more conserved DBLα
654 domains and an e-value of 1e-10 for the other domains. Next, the reads mapping to the different domains
655 were assembled separately. rnaSPAdes (read_error_correction on, k-mer = 15), Oases (kmer = 15) and
656 SoapDeNovo2 (kmer = 15) were all used to assemble the reads separately (Bushmanova *et al.*, 2019, Xie *et*
657 *al.*, 2014, Schulz *et al.*, 2012). The output of the different assemblers was combined into a per sample
658 reference of domain sequences. Redundancy was removed in the reference using cd-hit (-n 8-c 0.99) (at
659 sequence identity = 99%) (Fu *et al.*, 2012). Cap3 was used to merge and extend the domain assemblies (Huang
660 & Madan, 1999). SSPACE was used to join the domains together (parameters -n 31 -x 0 -k 10) (Boetzer *et al.*,
661 2011). Transcript annotation was performed as in the whole transcript approach, with transcripts < 500 nt
662 removed. Significantly annotated (1e-5) transcripts were identified and selected. The most significant
663 annotation was selected as the best annotation for each region, with multiple annotations allowed on a single
664 transcript if the regions were not overlapping. For both methods, a *var* transcript was selected if it contained
665 at least one significantly annotated domain (in exon 1). *Var* transcripts that encoded only the more conserved
666 exon 2 (acidic terminal segment (ATS) domain) were discarded.
667
668 <u>Validation on RNA-sequencing dataset from *P. falciparum* reference strain 3D7</u>
669 Both new approaches and the original approach (SoapDeNovo-Trans, k =71) (Wichers *et al.*, 2021, Tonkin-Hill
670 *et al.*, 2018) were run on a public RNA-sequencing dataset of the intra-erythrocytic life cycle stages of cultured
671 *P. falciparum* 3D7 strain, sampled at 8-hr intervals up until 40 hrs post infection and then at 4 hr intervals up
672 until 48 hrs post infection (ENA: PRJEB31535) (Wichers *et al.*, 2019). This provided a validation of all three
673 approaches due to the true sequence of the *var* genes being known in *P. falciparum* 3D7 strain. Therefore,
674 we compared the assembled sequences from all three approaches to the true sequence. The first best hit
675 (significance threshold = 1e-10) was chosen for each contig. The alignment score was used to evaluate the
676 performance of each method. The alignment score represents √accuracy* recovery. The accuracy is the
677 proportion of bases that are correct in the assembled transcript and the recovery reflects what proportion of
678 the true transcript was assembled. Misassemblies were counted as transcripts that had a percentage identity
679 < 99% to their best hit (i.e. the *var* transcript is not 100% contained against the reference).
680
681 <u>Comparison of approaches for *var* assembly on *ex vivo* samples</u>
682 The *var* transcripts assembled from the 32 *ex vivo* samples using the original approach were compared to
683 those produced from the whole transcript and domain assembly approaches. The whole transcript approach
684 was chosen for subsequent analysis and all assembled *var* transcripts from this approach were combined into
685 a reference, as in the original method (Wichers *et al.*, 2021).
686 Removal of *var* transcripts with sequence id >= 99% prior to mapping was not performed in the original
687 analysis. To overcome this, *var* transcripts were removed if they had a sequence id >= 99% against the full
688 complement in the whole transcript approach, using cd-hit-est (Fu *et al.*, 2012). Removing redundancy in the
689 reference of assembled *var* transcripts across all samples led to the removal of 1,316 assembled contigs
690 generated from the whole transcript approach.
691 This reference then represented all assembled *var* transcripts across all samples in the given analysis. The
692 same method that was used in the original analysis was applied for quantifying the expression of the
693 assembled *var* transcripts. The non-core reads were mapped against this reference and quantification was
694 performed using Salmon (Patro *et al.*, 2017). DESeq2 was used to perform differential expression analysis
695 between severe versus non-severe groups and naïve versus pre-exposed groups in the original analysis (Love
696 *et al.*, 2014). Here, the same approach, as used in the original analysis, was applied to see if concordant
697 expression estimates were obtained. As genomic sequencing was not available, this provided a confirmation
698 of the whole transcript approach after the domain annotation step. The assembled *var* transcripts produced
699 by the whole transcript assembly approach had their expression quantified at the transcript and domain level,
700 as in the original method, and the results were compared to those obtained by the original method. To

701 quantify domain expression, featureCounts was used, as in the original method with the counts for each
702 domain aggregated (Liao *et al.*, 2014). Correlation analysis between the domain's counts from the whole
703 transcript approach and the original method was performed for each *ex vivo* sample. Differential expression
704 analysis was also performed using DESeq2, as in the original analysis and the results compared (Love *et al.*,
705 2014, Wichers *et al.*, 2021).
706
707 Estimation of parasite lifecycle stage distribution in *ex vivo* and short-term *in vitro* samples
708 To determine the parasite life cycle stage proportions for each sample the mixture model approach of the
709 original analysis (Tonkin-Hill *et al.*, 2018, Wichers *et al.*, 2021) and the SCDC approach were used (Dong *et al.*,
710 2021, Howick *et al.*, 2019). Recently, it has been determined that species-agnostic reference datasets can be
711 used for efficient and accurate gene expression deconvolution of bulk RNA-sequencing data from any
712 *Plasmodium* species and for correct gene expression analyses for biases caused by differences in stage
713 composition among samples (Tebben *et al.*, 2022). Therefore, the *Plasmodium berghei* single cell atlas was
714 used as reference with restriction to 1:1 orthologs between *P. berghei* and *P. falciparum*. This reference was
715 chosen as it contained reference transcriptomes for the gametocyte stage. To ensure consistency with the
716 original analysis, proportions from the mixture model approach were used for all subsequent analyses
717 (Wichers *et al.*, 2021). For comparison, the proportion of different stages of the parasite life cycle in the *ex*
718 *vivo* and *in vitro* samples was determined by two independent readers in Giemsa-stained thin blood smears.
719 The same classification as the mixture model approach was used (8, 19, 30, and 42 hours post infection
720 corresponding to ring, early trophozoite, late trophozoite and schizont stages respectively). Significant
721 differences in ring stage proportions were tested using pairwise Wilcoxon tests. For the other stages, a
722 modified Wilcoxon rank test for zero-inflated data was used (Wang *et al.*, 2021). *Var* gene expression is highly
723 stage dependent, so any quantitative comparison between samples needs adjustment for developmental
724 stage. The life cycle stage proportions determined from the mixture model approach were used for
725 adjustment.
726
727 Characterising *var* transcripts
728 The whole transcript approach was applied to the paired *ex vivo* and *in vitro* samples. Significant differences
729 in the number of assembled *var* transcripts and the length of the transcripts across the generations was tested
730 using the paired Wilcoxon test. Redundancy was removed from the assembled *var* transcripts and transcripts
731 and domains were quantified using the approach described above. Three additional filtering steps were
732 applied separately to this reference of assembled *var* transcripts to ensure the *var* transcripts that went on to
733 have their expression quantified represented true *var* transcripts. The first method restricted *var* transcripts
734 to those greater than 1500nt containing at least 3 significantly annotated *var* domains, one of which had to
735 be a DBLα domain. The second restricted *var* transcripts to those greater than 1500nt and containing a DBLα
736 domain. The third approach restricted *var* transcripts to those greater than 1500nt with at least 3 significant
737 *var* domain annotations.
738
739 Per patient *var* transcript expression
740 A limitation of *var* transcript differential expression analysis is that it assumes all *var* sequences have the
741 possibility of being expressed in all samples. However, since each parasite isolate has a different set of *var*
742 gene sequences, this assumption is not completely valid. To account for this, *var* transcript expression analysis
743 was performed on a per patient basis. For each patient, the paired *ex vivo* and *in vitro* samples were analysed.
744 The assembled *var* transcripts (at least 1500nt and containing 3 significantly annotated *var* domains) across
745 all the generations for a patient were combined into a reference, redundancy was removed as described
746 above, and expression was quantified using Salmon (Patro *et al.*, 2017). *Var* transcript expression was ranked,
747 and the rankings compared across the generations.
748
749 *Var* expression homogeneity (VEH)

750 VEH is defined as the extent to which a small number of *var* gene sequences dominate an isolate's expression
751 profile (Warimwe *et al.*, 2013). Previously, this has been evaluated by calculating a commonly used α diversity
752 index, the Simpson's index of diversity. Different α diversity indexes put different weights on evenness and
753 richness. To overcome the issue of choosing one metric, α diversity curves were calculated (Wagner *et al.*,
754 2018). Equation 1 is the computational formula for diversity curves. *D* is calculated for *q* in the range 0 to 3
755 with a step increase of 0.1 and *p* in this analysis represented the proportion of *var* gene expression dedicated
756 to *var* transcript *k*. *q* determined how much weight is given to rare vs abundant *var* transcripts. The smaller
757 the *q* value, the less weight was given to the more abundant *var* transcript. VEH was investigated on a per
758 patient basis.
759
760
761 Equation 1 $$D_{(q)} = (\sum_{k=1}^{K} p_k^q)^{\frac{1}{1-q}}$$
762
763
764 Conserved *var* gene variants
765 To check for the differential expression of conserved *var* gene variants *var1-3D7*, *var1-IT* and *var2csa*, all
766 assembled transcripts significantly annotated as such were identified. For each conserved gene, Salmon
767 normalised read counts (adjusted for life cycle stage) were summed and expression compared across the
768 generations using a pairwise Wilcoxon rank test.
769
770 Differential expression of *var* domains from *ex vivo* to *in vitro* samples
771 Domain expression was quantified using featureCounts, as described above (Liao *et al.*, 2014). DESeq2 was
772 used to test for differential domain expression, with five expected read counts in at least three patient isolates
773 required, with life cycle stage and patient identity used as covariates. For the *ex vivo* versus *in vitro*
774 comparisons, only *ex vivo* samples that had paired samples in generation 1 underwent differential expression
775 analysis, given the extreme nature of the polymorphism seen in the *var* genes.
776
777 *Var* group expression analysis
778 The type of the *var* gene is determined by multiple parameters: upstream sequence (ups), chromosomal
779 location, direction of transcription and domain composition. All regular *var* genes encode a DBLα domain in
780 the N-terminus of the PfEMP1 protein (Figure 1c). The type of this domain correlates with previously defined
781 *var* gene groups, with group A encoding DBLα1, groups B and C encoding DBLα0 and group B encoding a
782 DBLα2 (chimera between DBLα0 and DBLα1) (Figure 1c). The DBLα domain sequence for each transcript was
783 determined and for each patient a reference of all assembled DBLα domains combined. The relevant sample's
784 non-core reads were mapped to this using Salmon and DBLα expression quantified (Patro *et al.*, 2017). DESeq2
785 normalisation was performed, with patient identity and life cycle stage proportions included as covariates and
786 differences in the amounts of *var* transcripts of group A compared with groups B and C assessed (Love *et al.*,
787 2014). A similar approach was repeated for NTS domains. NTSA domains are found encoded in group A *var*
788 genes and NTSB domains are found encoded in group B and C *var* genes (Figure 1c).
789
790 Quantification of total *var* gene expression
791 The RNA-sequencing reads were blastn (with the short-blastn option on and significance = 1e-10) against the
792 LARSFADIG nucleotide sequences (142 unique LARSFADIG sequences) to identify reads containing the
793 LARSFADIG motifs. This approach has been described previously (Andrade *et al.*, 2020). Once the reads
794 containing the LARSFADIG motifs had been identified, they were used to assembled the LARSFADIG motif.
795 Trinity (Henschel, 2012) and rnaSPAdes (Bushmanova *et al.*, 2019) were used separately to assemble the
796 LARSFADIG motif, and the results compared. The sequencing reads were mapped back against the assemblies
797 using bwa mem (Li, 2013), parameter -k 31 -a (as in Andrade *et al.*, 2020). Coverage over the LARSFADIG motif
798 was assessed by determining the coverage over the middle of the motif (S) using Samtools depth (Danecek *et*

799 *al.*, 2021). These values were divided by the number of reads mapped to the *var* exon 1 database and the 3D7
800 genome (which had *var* genes removed) to represent the proportion of total gene expression dedicated to
801 *var* gene expression (similar to an RPKM). The results of both approaches were compared. This method has
802 been validated on 3D7, IT and HB3 *Plasmodium* strains. *Var2csa* does not contain the LARSFADIG motif, hence
803 this quantitative analysis of global *var* gene expression excluded *var2csa* (which was analysed separately).
804 Significant differences in total *var* gene expression were tested by constructing a linear model with the
805 proportion of gene expression dedicated to *var* gene expression as the response variable, the generation and
806 life cycle stage as an independent variables and the patient identity included as a random effect.
807
808 *Var* expression profiling by DBLα-tag sequencing
809 DBLα-tag sequence analysis was performed as in the original analysis (Wichers *et al.*, 2021), with Varia used
810 to predict domain composition (Mackenzie *et al.*, 2022). The proportion of transcripts encoding NTSA, NTSB,
811 DBLα1, DBLα2 and DBLα0 domains were determined for each sample. These expression levels were used as
812 an alternative approach to see whether there were changes in the *var* group expression levels through culture.
813
814 The consistency of domain annotations was also investigated between the DBLα-tag approach and the
815 assembled transcripts. This was investigated on a per patient basis, with all the predicted annotations from
816 the DBLα-tag approach for a given patient combined. These were compared to the annotations from all
817 assembled transcripts for a given patient. DBLα annotations and DBLα-CIDR annotations were compared. This
818 provided another validation of the whole transcript approach after the domain annotation step and was not
819 dependent on performing differential expression analysis.
820
821 For comparison of both approaches (DBLα-tag sequencing and our new whole transcript approach), the same
822 analysis was performed as in the original analysis (Wichers *et al.*, 2021). All conserved variants (*var1, var2csa*
823 and *var3*) were removed as they were not properly amplified by the DBLα-tag approach. To identify how many
824 assembled transcripts, specifically the DBLα region, were found in the DBLα-tag approach, we applied BLAST.
825 As in the original analysis, a BLAST database was created from the DBLα-tag cluster results and screened for
826 the occurrence of those assembled DBLα regions with more than 97% seq id using the "megablast" option.
827 This was restricted to the assembled DBLα regions that were expressed in the top 75th percentile to allow for
828 a fair comparison, as only DBLα-tag clusters with more than 10 reads were considered. Similarly, to identify
829 how many DBLα-tag sequences were found in the assembled transcripts, a BLAST database was created from
830 the assembled transcripts and screened for the occurrence of the DBLα-tag sequences with more than 97%
831 seq id using the "megablast" option. This was performed for each sample.
832
833 Core gene differential expression analysis
834 Subread align was used, as in the original analysis, to align the reads to the human genome and *P. falciparum*
835 3D7 genome, *with var, rif, stevor, surf* and *rRNA* genes removed (Liao *et al.*, 2013). HTSeq count was used to
836 quantify gene counts (Anders *et al.*, 2015). DESeq2 was used to test for differentially expressed genes with
837 five read counts in at least three samples being required (Love *et al.*, 2014). Parasite life cycle stages and
838 patient identity were included as covariates. GO and KEGG analysis was performed using ShinyGo and
839 significant terms were defined by having a Bonferroni corrected p-value < 0.05 (Ge *et al.*, 2020).
840
841 Funding / Acknowledgements
842 CAB received support from the Wellcome Trust (4-Year PhD programme, grant number 220123/Z/20/Z).
843 Infrastructure support for this research was provided by the NIHR Imperial Biomedical Research Centre and
844 Imperial College Research Computing Service, DOI: 10.14469/hpc/2232.
845 JSWM, YDH and AB were funded by the German Research Foundation (DFG) grants BA 5213/3-1 (project
846 #323759012) and BA 5213/6-1 (project #433302244).

847 TO is supported by the Wellcome Trust grant 104111/Z/14/ZR. The funders had no role in study design, data
848 collection and analysis, decision to publish, or preparation of the manuscript.
849 JB acknowledges support from Wellcome (100993/Z/13/Z)
850

851 Author contribution
852 Conceptualization: CAB, TDO, AB, AJC
853 Methodology: CAB, MFD, TL, TDO
854 Software: CAB
855 Validation: CAB, AB
856 Formal analysis: CAB
857 Investigation: JSW, HvT, YDH, JAMS, HSH, EFH, AB
858 Resources: TL, AJC, AB
859 Data curation: CAB, AB
860 Writing – original draft: CAB, TDO, AJC, AB
861 Writing – review & editing: CAB, JSW, MFD, TL, TWG, JB, TDO, AJC, AB
862 Visualization: CAB
863 Supervision: TWG, JB, TDO, AJC, AB
864 Project Administration: CAB, AJC, AB
865 Funding acquisition: AJC, AB
866
867 All authors read and approved the manuscript.
868

869 Competing interests
870 No competing interests declared.
871

872 References
873 Almelli, T., Nuel, G., Bischoff, E., Aubouy, A., Elati, M., Wang, C.W., Dillies, M.A., Coppee, J.Y., Ayissi, G.N.,
874 Basco, L.K., Rogier, C., Ndam, N.T., Deloron, P., and Tahar, R. (2014) Differences in gene transcriptomic
875 pattern of Plasmodium falciparum in children with cerebral malaria and asymptomatic carriers. *PLoS*
876 *One* **9**: e114401.
877 Anders, S., Pyl, P.T., and Huber, W. (2015) HTSeq--a Python framework to work with high-throughput
878 sequencing data. *Bioinformatics* **31**: 166-169.
879 Andrade, C.M., Fleckenstein, H., Thomson-Luque, R., Doumbo, S., Lima, N.F., Anderson, C., Hibbert, J., Hopp,
880 C.S., Tran, T.M., Li, S., Niangaly, M., Cisse, H., Doumtabe, D., Skinner, J., Sturdevant, D., Ricklefs, S.,
881 Virtaneva, K., Asghar, M., Homann, M.V., Turner, L., Martins, J., Allman, E.L., N'Dri, M.E., Winkler, V.,
882 Llinas, M., Lavazec, C., Martens, C., Farnert, A., Kayentao, K., Ongoiba, A., Lavstsen, T., Osorio, N.S.,
883 Otto, T.D., Recker, M., Traore, B., Crompton, P.D., and Portugal, S. (2020) Increased circulation time of
884 Plasmodium falciparum underlies persistent asymptomatic infection in the dry season. *Nat Med* **26**:
885 1929-1940.
886 Andreadaki, M., Pace, T., Grasso, F., Siden-Kiamos, I., Mochi, S., Picci, L., Bertuccini, L., Ponzi, M., and Curra,
887 C. (2020) Plasmodium berghei Gamete Egress Protein is required for fertility of both genders.
888 *Microbiologyopen* **9**: e1038.
889 Avril, M., Tripathi, A.K., Brazier, A.J., Andisi, C., Janes, J.H., Soma, V.L., Sullivan, D.J., Jr., Bull, P.C., Stins, M.F.,
890 and Smith, J.D. (2012) A restricted subset of var genes mediates adherence of Plasmodium falciparum-
891 infected erythrocytes to brain endothelial cells. *Proc Natl Acad Sci U S A* **109**: E1782-1790.
892 Bachmann, A., Predehl, S., May, J., Harder, S., Burchard, G.D., Gilberger, T.W., Tannich, E., and Bruchhaus, I.
893 (2011) Highly co-ordinated var gene expression and switching in clinical Plasmodium falciparum
894 isolates from non-immune malaria patients. *Cell Microbiol* **13**: 1397-1409.

895 Baruch, D.I., Pasloske, B.L., Singh, H.B., Bi, X., Ma, X.C., Feldman, M., Taraschi, T.F., and Howard, R.J. (1995)
896 Cloning the P. falciparum gene encoding PfEMP1, a malarial variant antigen and adherence receptor
897 on the surface of parasitized human erythrocytes. *Cell* **82**: 77-87.
898 Beeson, J.G., Drew, D.R., Boyle, M.J., Feng, G., Fowkes, F.J., and Richards, J.S. (2016) Merozoite surface
899 proteins in red blood cell invasion, immunity and vaccines against malaria. *FEMS Microbiol Rev* **40**:
900 343-372.
901 Bernabeu, M., Danziger, S.A., Avril, M., Vaz, M., Babar, P.H., Brazier, A.J., Herricks, T., Maki, J.N., Pereira, L.,
902 Mascarenhas, A., Gomes, E., Chery, L., Aitchison, J.D., Rathod, P.K., and Smith, J.D. (2016) Severe adult
903 malaria is associated with specific PfEMP1 adhesion types and high parasite biomass. *Proc Natl Acad*
904 *Sci U S A* **113**: E3270-3279.
905 Boetzer, M., Henkel, C.V., Jansen, H.J., Butler, D., and Pirovano, W. (2011) Scaffolding pre-assembled contigs
906 using SSPACE. *Bioinformatics* **27**: 578-579.
907 Bozdech, Z., Llinas, M., Pulliam, B.L., Wong, E.D., Zhu, J., and DeRisi, J.L. (2003) The transcriptome of the
908 intraerythrocytic developmental cycle of Plasmodium falciparum. *PLoS Biol* **1**: E5.
909 Brown, A.C., and Guler, J.L. (2020) From Circulation to Cultivation: Plasmodium In Vivo versus In Vitro. *Trends*
910 *Parasitol* **36**: 914-926.
911 Bruske, E.I., Dimonte, S., Enderes, C., Tschan, S., Flotenmeyer, M., Koch, I., Berger, J., Kremsner, P., and Frank,
912 M. (2016) In Vitro Variant Surface Antigen Expression in Plasmodium falciparum Parasites from a Semi-
913 Immune Individual Is Not Correlated with Var Gene Transcription. *PLoS One* **11**: e0166135.
914 Bushmanova, E., Antipov, D., Lapidus, A., and Prjibelski, A.D. (2019) rnaSPAdes: a de novo transcriptome
915 assembler and its application to RNA-Seq data. *Gigascience* **8**.
916 Carrington, E., Cooijmans, R.H.M., Keller, D., Toenhake, C.G., Bartfai, R., and Voss, T.S. (2021) The ApiAP2
917 factor PfAP2-HC is an integral component of heterochromatin in the malaria parasite Plasmodium
918 falciparum. *iScience* **24**: 102444.
919 Claessens, A., Adams, Y., Ghumra, A., Lindergard, G., Buchan, C.C., Andisi, C., Bull, P.C., Mok, S., Gupta, A.P.,
920 Wang, C.W., Turner, L., Arman, M., Raza, A., Bozdech, Z., and Rowe, J.A. (2012) A subset of group A-
921 like var genes encodes the malaria parasite ligands for binding to human brain endothelial cells. *Proc*
922 *Natl Acad Sci U S A* **109**: E1772-1781.
923 Claessens, A., Affara, M., Assefa, S.A., Kwiatkowski, D.P., and Conway, D.J. (2017) Culture adaptation of malaria
924 parasites selects for convergent loss-of-function mutants. *Sci Rep* **7**: 41303.
925 Danecek, P., Bonfield, J.K., Liddle, J., Marshall, J., Ohan, V., Pollard, M.O., Whitwham, A., Keane, T., McCarthy,
926 S.A., Davies, R.M., and Li, H. (2021) Twelve years of SAMtools and BCFtools. *Gigascience* **10**.
927 Dimonte, S., Bruske, E.I., Hass, J., Supan, C., Salazar, C.L., Held, J., Tschan, S., Esen, M., Flotenmeyer, M., Koch,
928 I., Berger, J., Bachmann, A., Sim, B.K., Hoffman, S.L., Kremsner, P.G., Mordmuller, B., and Frank, M.
929 (2016) Sporozoite Route of Infection Influences In Vitro var Gene Transcription of Plasmodium
930 falciparum Parasites From Controlled Human Infections. *J Infect Dis* **214**: 884-894.
931 Dong, M., Thennavan, A., Urrutia, E., Li, Y., Perou, C.M., Zou, F., and Jiang, Y. (2021) SCDC: bulk gene expression
932 deconvolution by multiple single-cell RNA sequencing references. *Brief Bioinform* **22**: 416-427.
933 Finn, R.D., Clements, J., and Eddy, S.R. (2011) HMMER web server: interactive sequence similarity searching.
934 *Nucleic Acids Res* **39**: W29-37.
935 Fu, L., Niu, B., Zhu, Z., Wu, S., and Li, W. (2012) CD-HIT: accelerated for clustering the next-generation
936 sequencing data. *Bioinformatics* **28**: 3150-3152.
937 Ge, S.X., Jung, D., and Yao, R. (2020) ShinyGO: a graphical gene-set enrichment tool for animals and plants.
938 *Bioinformatics* **36**: 2628-2629.
939 Guillochon, E., Fraering, J., Joste, V., Kamaliddin, C., Vianou, B., Houze, L., Baudrin, L.G., Faucher, J.F., Aubouy,
940 A., Houze, S., Cot, M., Argy, N., Taboureau, O., Bertin, G.I., and Neuro, C.M.g. (2022) Transcriptome
941 Analysis of Plasmodium falciparum Isolates From Benin Reveals Specific Gene Expression Associated
942 With Cerebral Malaria. *J Infect Dis* **225**: 2187-2196.

943 Henschel, R., Lieber, M., Wu, L., Nista, P. M., Haas, B. J., LeDuc, R. D., (2012) Trinity RNA-Seq assembler
944 performance optimization. In: XSEDE '12: Proceedings of the 1st Conference of the Extreme Science
945 and Engineering Discovery Environment: Bridging from the eXtreme to the campus and beyond. ACM,
946 pp. 1-8.
947 Hoo, R., Bruske, E., Dimonte, S., Zhu, L., Mordmuller, B., Sim, B.K.L., Kremsner, P.G., Hoffman, S.L., Bozdech,
948 Z., Frank, M., and Preiser, P.R. (2019) Transcriptome profiling reveals functional variation in
949 Plasmodium falciparum parasites from controlled human malaria infection studies. *EBioMedicine* **48**:
950 442-452.
951 Howick, V.M., Russell, A.J.C., Andrews, T., Heaton, H., Reid, A.J., Natarajan, K., Butungi, H., Metcalf, T., Verzier,
952 L.H., Rayner, J.C., Berriman, M., Herren, J.K., Billker, O., Hemberg, M., Talman, A.M., and Lawniczak,
953 M.K.N. (2019) The Malaria Cell Atlas: Single parasite transcriptomes across the complete Plasmodium
954 life cycle. *Science* **365**.
955 Huang, X., and Madan, A. (1999) CAP3: A DNA sequence assembly program. *Genome Res* **9**: 868-877.
956 Jensen, A.T., Magistrado, P., Sharp, S., Joergensen, L., Lavstsen, T., Chiucchiuini, A., Salanti, A., Vestergaard,
957 L.S., Lusingu, J.P., Hermsen, R., Sauerwein, R., Christensen, J., Nielsen, M.A., Hviid, L., Sutherland, C.,
958 Staalsoe, T., and Theander, T.G. (2004) Plasmodium falciparum associated with severe childhood
959 malaria preferentially expresses PfEMP1 encoded by group A var genes. *J Exp Med* **199**: 1179-1190.
960 Jespersen, J.S., Wang, C.W., Mkumbaye, S.I., Minja, D.T., Petersen, B., Turner, L., Petersen, J.E., Lusingu, J.P.,
961 Theander, T.G., and Lavstsen, T. (2016) Plasmodium falciparum var genes expressed in children with
962 severe malaria encode CIDRalpha1 domains. *EMBO Mol Med* **8**: 839-850.
963 Joste, V., Guillochon, E., Fraering, J., Vianou, B., Watier, L., Jafari-Guemouri, S., Cot, M., Houze, S., Aubouy, A.,
964 Faucher, J.F., Argy, N., and Bertin, G.I. (2020) PfEMP1 A-Type ICAM-1-Binding Domains Are Not
965 Associated with Cerebral Malaria in Beninese Children. *mBio* **11**.
966 Kaneko, I., Iwanaga, S., Kato, T., Kobayashi, I., and Yuda, M. (2015) Genome-Wide Identification of the Target
967 Genes of AP2-O, a Plasmodium AP2-Family Transcription Factor. *PLoS Pathog* **11**: e1004905.
968 Kessler, A., Dankwa, S., Bernabeu, M., Harawa, V., Danziger, S.A., Duffy, F., Kampondeni, S.D., Potchen, M.J.,
969 Dambrauskas, N., Vigdorovich, V., Oliver, B.G., Hochman, S.E., Mowrey, W.B., MacCormick, I.J.C.,
970 Mandala, W.L., Rogerson, S.J., Sather, D.N., Aitchison, J.D., Taylor, T.E., Seydel, K.B., Smith, J.D., and
971 Kim, K. (2017) Linking EPCR-Binding PfEMP1 to Brain Swelling in Pediatric Cerebral Malaria. *Cell Host*
972 *Microbe* **22**: 601-614 e605.
973 Kirchgatter, K., and Portillo Hdel, A. (2002) Association of severe noncerebral Plasmodium falciparum malaria
974 in Brazil with expressed PfEMP1 DBL1 alpha sequences lacking cysteine residues. *Mol Med* **8**: 16-23.
975 Kraemer, S.M., and Smith, J.D. (2003) Evidence for the importance of genetic structuring to the structural and
976 functional specialization of the Plasmodium falciparum var gene family. *Mol Microbiol* **50**: 1527-1538.
977 Kyes, S.A., Kraemer, S.M., and Smith, J.D. (2007) Antigenic variation in Plasmodium falciparum: gene
978 organization and regulation of the var multigene family. *Eukaryot Cell* **6**: 1511-1520.
979 Lavstsen, T., Magistrado, P., Hermsen, C.C., Salanti, A., Jensen, A.T., Sauerwein, R., Hviid, L., Theander, T.G.,
980 and Staalsoe, T. (2005) Expression of Plasmodium falciparum erythrocyte membrane protein 1 in
981 experimentally infected humans. *Malar J* **4**: 21.
982 Lavstsen, T., Salanti, A., Jensen, A.T., Arnot, D.E., and Theander, T.G. (2003) Sub-grouping of Plasmodium
983 falciparum 3D7 var genes based on sequence analysis of coding and non-coding regions. *Malar J* **2**: 27.
984 Lavstsen, T., Turner, L., Saguti, F., Magistrado, P., Rask, T.S., Jespersen, J.S., Wang, C.W., Berger, S.S., Baraka,
985 V., Marquard, A.M., Seguin-Orlando, A., Willerslev, E., Gilbert, M.T., Lusingu, J., and Theander, T.G.
986 (2012) Plasmodium falciparum erythrocyte membrane protein 1 domain cassettes 8 and 13 are
987 associated with severe malaria in children. *Proc Natl Acad Sci U S A* **109**: E1791-1800.
988 Lee, H.J., Georgiadou, A., Walther, M., Nwakanma, D., Stewart, L.B., Levin, M., Otto, T.D., Conway, D.J., Coin,
989 L.J., and Cunnington, A.J. (2018) Integrated pathogen load and dual transcriptome analysis of systemic
990 host-pathogen interactions in severe malaria. *Sci Transl Med* **10**.

991 Leech, J.H., Barnwell, J.W., Miller, L.H., and Howard, R.J. (1984) Identification of a strain-specific malarial
992 antigen exposed on the surface of Plasmodium falciparum-infected erythrocytes. *J Exp Med* **159**:
993 1567-1575.
994 Lewis, T.E., Sillitoe, I., and Lees, J.G. (2019) cath-resolve-hits: a new tool that resolves domain matches
995 suspiciously quickly. *Bioinformatics* **35**: 1766-1767.
996 Li, H. (2013) Aligning sequence reads, clone sequences and assembly contigs with BWA-MEM. *arXiv*:
997 1303.3997v1301 [q-bio.GN].
998 Liao, Y., Smyth, G.K., and Shi, W. (2013) The Subread aligner: fast, accurate and scalable read mapping by
999 seed-and-vote. *Nucleic Acids Res* **41**: e108.
000 Liao, Y., Smyth, G.K., and Shi, W. (2014) featureCounts: an efficient general purpose program for assigning
001 sequence reads to genomic features. *Bioinformatics* **30**: 923-930.
002 Lischer, H.E.L., and Shimizu, K.K. (2017) Reference-guided de novo assembly approach improves genome
003 reconstruction for related species. *BMC Bioinformatics* **18**: 474.
004 Love, M.I., Huber, W., and Anders, S. (2014) Moderated estimation of fold change and dispersion for RNA-seq
005 data with DESeq2. *Genome Biol* **15**: 550.
006 Mackenzie, G., Jensen, R.W., Lavstsen, T., and Otto, T.D. (2022) Varia: a tool for prediction, analysis and
007 visualisation of variable genes. *BMC Bioinformatics* **23**: 52.
008 Mackinnon, M.J., Li, J., Mok, S., Kortok, M.M., Marsh, K., Preiser, P.R., and Bozdech, Z. (2009) Comparative
009 transcriptional and genomic analysis of Plasmodium falciparum field isolates. *PLoS Pathog* **5**:
010 e1000644.
011 MalariaGen, Ahouidi, A., Ali, M., Almagro-Garcia, J., Amambua-Ngwa, A., Amaratunga, C., Amato, R., Amenga-
012 Etego, L., Andagalu, B., Anderson, T.J.C., Andrianaranjaka, V., Apinjoh, T., Ariani, C., Ashley, E.A.,
013 Auburn, S., Awandare, G.A., Ba, H., Baraka, V., Barry, A.E., Bejon, P., Bertin, G.I., Boni, M.F., Borrmann,
014 S., Bousema, T., Branch, O., Bull, P.C., Busby, G.B.J., Chookajorn, T., Chotivanich, K., Claessens, A.,
015 Conway, D., Craig, A., D'Alessandro, U., Dama, S., Day, N.P., Denis, B., Diakite, M., Djimde, A., Dolecek,
016 C., Dondorp, A.M., Drakeley, C., Drury, E., Duffy, P., Echeverry, D.F., Egwang, T.G., Erko, B., Fairhurst,
017 R.M., Faiz, A., Fanello, C.A., Fukuda, M.M., Gamboa, D., Ghansah, A., Golassa, L., Goncalves, S.,
018 Hamilton, W.L., Harrison, G.L.A., Hart, L., Henrichs, C., Hien, T.T., Hill, C.A., Hodgson, A., Hubbart, C.,
019 Imwong, M., Ishengoma, D.S., Jackson, S.A., Jacob, C.G., Jeffery, B., Jeffreys, A.E., Johnson, K.J., Jyothi,
020 D., Kamaliddin, C., Kamau, E., Kekre, M., Kluczynski, K., Kochakarn, T., Konate, A., Kwiatkowski, D.P.,
021 Kyaw, M.P., Lim, P., Lon, C., Loua, K.M., Maiga-Ascofare, O., Malangone, C., Manske, M., Marfurt, J.,
022 Marsh, K., Mayxay, M., Miles, A., Miotto, O., Mobegi, V., Mokuolu, O.A., Montgomery, J., Mueller, I.,
023 Newton, P.N., Nguyen, T., Nguyen, T.N., Noedl, H., Nosten, F., Noviyanti, R., Nzila, A.*, et al.* (2021) An
024 open dataset of Plasmodium falciparum genome variation in 7,000 worldwide samples. *Wellcome*
025 *Open Res* **6**: 42.
026 Mkumbaye, S.I., Wang, C.W., Lyimo, E., Jespersen, J.S., Manjurano, A., Mosha, J., Kavishe, R.A., Mwakalinga,
027 S.B., Minja, D.T.R., Lusingu, J.P., Theander, T.G., and Lavstsen, T. (2017) The Severity of Plasmodium
028 falciparum Infection Is Associated with Transcript Levels of var Genes Encoding Endothelial Protein C
029 Receptor-Binding P. falciparum Erythrocyte Membrane Protein 1. *Infect Immun* **85**.
030 Mok, B.W., Ribacke, U., Rasti, N., Kironde, F., Chen, Q., Nilsson, P., and Wahlgren, M. (2008) Default Pathway
031 of var2csa switching and translational repression in Plasmodium falciparum. *PLoS One* **3**: e1982.
032 Oakley, M.S., Kumar, S., Anantharaman, V., Zheng, H., Mahajan, B., Haynes, J.D., Moch, J.K., Fairhurst, R.,
033 McCutchan, T.F., and Aravind, L. (2007) Molecular factors and biochemical pathways induced by
034 febrile temperature in intraerythrocytic Plasmodium falciparum parasites. *Infect Immun* **75**: 2012-
035 2025.
036 Otto, T.D., Assefa, S.A., Bohme, U., Sanders, M.J., Kwiatkowski, D., Pf3k, c., Berriman, M., and Newbold, C.
037 (2019) Evolutionary analysis of the most polymorphic gene family in falciparum malaria. *Wellcome*
038 *Open Res* **4**: 193.

039 Patro, R., Duggal, G., Love, M.I., Irizarry, R.A., and Kingsford, C. (2017) Salmon provides fast and bias-aware
040 quantification of transcript expression. *Nat Methods* **14**: 417-419.
041 Peters, J.M., Fowler, E.V., Krause, D.R., Cheng, Q., and Gatton, M.L. (2007) Differential changes in Plasmodium
042 falciparum var transcription during adaptation to culture. *J Infect Dis* **195**: 748-755.
043 Pickford, A.K., Michel-Todo, L., Dupuy, F., Mayor, A., Alonso, P.L., Lavazec, C., and Cortes, A. (2021) Expression
044 Patterns of Plasmodium falciparum Clonally Variant Genes at the Onset of a Blood Infection in Malaria-
045 Naive Humans. *mBio* **12**: e0163621.
046 Quintana, M.D.P., Ecklu-Mensah, G., Tcherniuk, S.O., Ditlev, S.B., Oleinikov, A.V., Hviid, L., and Lopez-Perez,
047 M. (2019) Comprehensive analysis of Fc-mediated IgM binding to the Plasmodium falciparum
048 erythrocyte membrane protein 1 family in three parasite clones. *Sci Rep* **9**: 6050.
049 Rask, T.S., Hansen, D.A., Theander, T.G., Gorm Pedersen, A., and Lavstsen, T. (2010) Plasmodium falciparum
050 erythrocyte membrane protein 1 diversity in seven genomes--divide and conquer. *PLoS Comput Biol*
051 **6**.
052 Robert, F., Ntoumi, F., Angel, G., Candito, D., Rogier, C., Fandeur, T., Sarthou, J.L., and Mercereau-Puijalon, O.
053 (1996) Extensive genetic diversity of Plasmodium falciparum isolates collected from patients with
054 severe malaria in Dakar, Senegal. *Trans R Soc Trop Med Hyg* **90**: 704-711.
055 Rorick, M.M., Rask, T.S., Baskerville, E.B., Day, K.P., and Pascual, M. (2013) Homology blocks of Plasmodium
056 falciparum var genes and clinically distinct forms of severe malaria in a local population. *BMC Microbiol*
057 **13**: 244.
058 Sahu, P.K., Duffy, F.J., Dankwa, S., Vishnyakova, M., Majhi, M., Pirpamer, L., Vigdorovich, V., Bage, J.,
059 Maharana, S., Mandala, W., Rogerson, S.J., Seydel, K.B., Taylor, T.E., Kim, K., Sather, D.N., Mohanty, A.,
060 Mohanty, R.R., Mohanty, A., Pattnaik, R., Aitchison, J.D., Hoffmann, A., Mohanty, S., Smith, J.D.,
061 Bernabeu, M., and Wassmer, S.C. (2021) Determinants of brain swelling in pediatric and adult cerebral
062 malaria. *JCI Insight* **6**.
063 Salanti, A., Dahlback, M., Turner, L., Nielsen, M.A., Barfod, L., Magistrado, P., Jensen, A.T., Lavstsen, T., Ofori,
064 M.F., Marsh, K., Hviid, L., and Theander, T.G. (2004) Evidence for the involvement of VAR2CSA in
065 pregnancy-associated malaria. *J Exp Med* **200**: 1197-1203.
066 Scherf, A., Hernandez-Rivas, R., Buffet, P., Bottius, E., Benatar, C., Pouvelle, B., Gysin, J., and Lanzer, M. (1998)
067 Antigenic variation in malaria: in situ switching, relaxed and mutually exclusive transcription of var
068 genes during intra-erythrocytic development in Plasmodium falciparum. *EMBO J* **17**: 5418-5426.
069 Schulz, M.H., Zerbino, D.R., Vingron, M., and Birney, E. (2012) Oases: robust de novo RNA-seq assembly across
070 the dynamic range of expression levels. *Bioinformatics* **28**: 1086-1092.
071 Shabani, E., Hanisch, B., Opoka, R.O., Lavstsen, T., and John, C.C. (2017) Plasmodium falciparum EPCR-binding
072 PfEMP1 expression increases with malaria disease severity and is elevated in retinopathy negative
073 cerebral malaria. *BMC Med* **15**: 183.
074 Smith, J.D., Chitnis, C.E., Craig, A.G., Roberts, D.J., Hudson-Taylor, D.E., Peterson, D.S., Pinches, R., Newbold,
075 C.I., and Miller, L.H. (1995) Switches in expression of Plasmodium falciparum var genes correlate with
076 changes in antigenic and cytoadherent phenotypes of infected erythrocytes. *Cell* **82**: 101-110.
077 Stevenson, L., Laursen, E., Cowan, G.J., Bandoh, B., Barfod, L., Cavanagh, D.R., Andersen, G.R., and Hviid, L.
078 (2015) alpha2-Macroglobulin Can Crosslink Multiple Plasmodium falciparum Erythrocyte Membrane
079 Protein 1 (PfEMP1) Molecules and May Facilitate Adhesion of Parasitized Erythrocytes. *PLoS Pathog*
080 **11**: e1005022.
081 Storm, J., Jespersen, J.S., Seydel, K.B., Szestak, T., Mbewe, M., Chisala, N.V., Phula, P., Wang, C.W., Taylor, T.E.,
082 Moxon, C.A., Lavstsen, T., and Craig, A.G. (2019) Cerebral malaria is associated with differential
083 cytoadherence to brain endothelial cells. *EMBO Mol Med* **11**.
084 Su, X.Z., Heatwole, V.M., Wertheimer, S.P., Guinet, F., Herrfeldt, J.A., Peterson, D.S., Ravetch, J.A., and
085 Wellems, T.E. (1995) The large diverse gene family var encodes proteins involved in cytoadherence
086 and antigenic variation of Plasmodium falciparum-infected erythrocytes. *Cell* **82**: 89-100.

087 Tarr, S.J., Diaz-Ingelmo, O., Stewart, L.B., Hocking, S.E., Murray, L., Duffy, C.W., Otto, T.D., Chappell, L., Rayner,
088 J.C., Awandare, G.A., and Conway, D.J. (2018) Schizont transcriptome variation among clinical isolates
089 and laboratory-adapted clones of the malaria parasite Plasmodium falciparum. *BMC Genomics* **19**:
090 894.
091 Taylor, H.M., Grainger, M., and Holder, A.A. (2002) Variation in the expression of a Plasmodium falciparum
092 protein family implicated in erythrocyte invasion. *Infect Immun* **70**: 5779-5789.
093 Tebben, K., Dia, A., and Serre, D. (2022) Determination of the Stage Composition of Plasmodium Infections
094 from Bulk Gene Expression Data. *mSystems* **7**: e0025822.
095 Tonkin-Hill, G.Q., Trianty, L., Noviyanti, R., Nguyen, H.H.T., Sebayang, B.F., Lampah, D.A., Marfurt, J., Cobbold,
096 S.A., Rambhatla, J.S., McConville, M.J., Rogerson, S.J., Brown, G.V., Day, K.P., Price, R.N., Anstey, N.M.,
097 Papenfuss, A.T., and Duffy, M.F. (2018) The Plasmodium falciparum transcriptome in severe malaria
098 reveals altered expression of genes involved in important processes including surface antigen-
099 encoding var genes. *PLoS Biol* **16**: e2004328.
100 Tuikue Ndam, N., Moussiliou, A., Lavstsen, T., Kamaliddin, C., Jensen, A.T.R., Mama, A., Tahar, R., Wang, C.W.,
101 Jespersen, J.S., Alao, J.M., Gamain, B., Theander, T.G., and Deloron, P. (2017) Parasites Causing
102 Cerebral Falciparum Malaria Bind Multiple Endothelial Receptors and Express EPCR and ICAM-1-
103 Binding PfEMP1. *J Infect Dis* **215**: 1918-1925.
104 Turner, L., Lavstsen, T., Berger, S.S., Wang, C.W., Petersen, J.E., Avril, M., Brazier, A.J., Freeth, J., Jespersen,
105 J.S., Nielsen, M.A., Magistrado, P., Lusingu, J., Smith, J.D., Higgins, M.K., and Theander, T.G. (2013)
106 Severe malaria is associated with parasite binding to endothelial protein C receptor. *Nature* **498**: 502-
107 505.
108 Ukaegbu, U.E., Kishore, S.P., Kwiatkowski, D.L., Pandarinath, C., Dahan-Pasternak, N., Dzikowski, R., and
109 Deitsch, K.W. (2014) Recruitment of PfSET2 by RNA polymerase II to variant antigen encoding loci
110 contributes to antigenic variation in P. falciparum. *PLoS Pathog* **10**: e1003854.
111 Ukaegbu, U.E., Zhang, X., Heinberg, A.R., Wele, M., Chen, Q., and Deitsch, K.W. (2015) A Unique Virulence
112 Gene Occupies a Principal Position in Immune Evasion by the Malaria Parasite Plasmodium falciparum.
113 *PLoS Genet* **11**: e1005234.
114 Vignali, M., Armour, C.D., Chen, J., Morrison, R., Castle, J.C., Biery, M.C., Bouzek, H., Moon, W., Babak, T.,
115 Fried, M., Raymond, C.K., and Duffy, P.E. (2011) NSR-seq transcriptional profiling enables identification
116 of a gene signature of Plasmodium falciparum parasites infecting children. *J Clin Invest* **121**: 1119-
117 1129.
118 Wagner, B.D., Grunwald, G.K., Zerbe, G.O., Mikulich-Gilbertson, S.K., Robertson, C.E., Zemanick, E.T., and
119 Harris, J.K. (2018) On the Use of Diversity Measures in Longitudinal Sequencing Studies of Microbial
120 Communities. *Front Microbiol* **9**: 1037.
121 Wahlgren, M., Goel, S., and Akhouri, R.R. (2017) Variant surface antigens of Plasmodium falciparum and their
122 roles in severe malaria. *Nat Rev Microbiol* **15**: 479-491.
123 Wang, W., Chen, E.Z., and Li, H. (2021) Truncated Rank-Based Tests for Two-Part Models with Excessive Zeros
124 and Applications to Microbiome Data. *arXiv*.
125 Warimwe, G.M., Recker, M., Kiragu, E.W., Buckee, C.O., Wambua, J., Musyoki, J.N., Marsh, K., and Bull, P.C.
126 (2013) Plasmodium falciparum var gene expression homogeneity as a marker of the host-parasite
127 relationship under different levels of naturally acquired immunity to malaria. *PLoS One* **8**: e70467.
128 WHO, (2022) World malaria report 2022. In. Geneva, pp.
129 Wichers, J.S., Scholz, J.A.M., Strauss, J., Witt, S., Lill, A., Ehnold, L.I., Neupert, N., Liffner, B., Luhken, R., Petter,
130 M., Lorenzen, S., Wilson, D.W., Low, C., Lavazec, C., Bruchhaus, I., Tannich, E., Gilberger, T.W., and
131 Bachmann, A. (2019) Dissecting the Gene Expression, Localization, Membrane Topology, and Function
132 of the Plasmodium falciparum STEVOR Protein Family. *mBio* **10**.
133 Wichers, J.S., Tonkin-Hill, G., Thye, T., Krumkamp, R., Kreuels, B., Strauss, J., von Thien, H., Scholz, J.A.,
134 Smedegaard Hansson, H., Weisel Jensen, R., Turner, L., Lorenz, F.R., Schollhorn, A., Bruchhaus, I.,
135 Tannich, E., Fendel, R., Otto, T.D., Lavstsen, T., Gilberger, T.W., Duffy, M.F., and Bachmann, A. (2021)

136 Common virulence gene expression in adult first-time infected malaria patients and severe cases. *Elife*
137 **10**.
138 Xie, Y., Wu, G., Tang, J., Luo, R., Patterson, J., Liu, S., Huang, W., He, G., Gu, S., Li, S., Zhou, X., Lam, T.W., Li, Y.,
139 Xu, X., Wong, G.K., and Wang, J. (2014) SOAPdenovo-Trans: de novo transcriptome assembly with
140 short RNA-Seq reads. *Bioinformatics* **30**: 1660-1666.
141 Yamagishi, J., Natori, A., Tolba, M.E., Mongan, A.E., Sugimoto, C., Katayama, T., Kawashima, S., Makalowski,
142 W., Maeda, R., Eshita, Y., Tuda, J., and Suzuki, Y. (2014) Interactive transcriptome analysis of malaria
143 patients and infecting Plasmodium falciparum. *Genome Res* **24**: 1433-1444.
144 Yang, X., Charlebois, P., Gnerre, S., Coole, M.G., Lennon, N.J., Levin, J.Z., Qu, J., Ryan, E.M., Zody, M.C., and
145 Henn, M.R. (2012) De novo assembly of highly diverse viral populations. *BMC Genomics* **13**: 475.
146 Yuda, M., Iwanaga, S., Shigenobu, S., Kato, T., and Kaneko, I. (2010) Transcription factor AP2-Sp and its target
147 genes in malarial sporozoites. *Mol Microbiol* **75**: 854-863.
148 Zerbino, D.R., and Birney, E. (2008) Velvet: algorithms for de novo short read assembly using de Bruijn graphs.
149 *Genome Res* **18**: 821-829.
150 Zhang, Q., Zhang, Y., Huang, Y., Xue, X., Yan, H., Sun, X., Wang, J., McCutchan, T.F., and Pan, W. (2011) From
151 in vivo to in vitro: dynamic analysis of Plasmodium falciparum var gene expression patterns of patient
152 isolates during adaptation to culture. *PLoS One* **6**: e20591.
153 Zhang, X., Florini, F., Visone, J.E., Lionardi, I., Gross, M.R., Patel, V., and Deitsch, K.W. (2022) A coordinated
154 transcriptional switching network mediates antigenic variation of human malaria parasites. *Elife* **11**.
155 Zimin, A.V., Marcais, G., Puiu, D., Roberts, M., Salzberg, S.L., and Yorke, J.A. (2013) The MaSuRCA genome
156 assembler. *Bioinformatics* **29**: 2669-2677.
157